Discrete Nonholonomic LL Systems on Lie Groups *

Yuri N. Fedorov
Department of Mathematics and Mechanics
Moscow Lomonosov University, Moscow, 119 899, Russia
e-mail: fedorov@mech.math.msu.su
and
Department de Matemàtica I,
Universitat Politecnica de Catalunya,
Barcelona, E-08028 Spain
e-mail: Yuri.Fedorov@upc.es
and
Dmitry V. Zenkov
Department of Mathematics
North Carolina State university
Raleigh, NC 27695
e-mail: dvzenkov@unity.ncsu.edu

September 21, 2004

Abstract

This paper applies the recently developed theory of discrete nonholonomic mechanics to the study of discrete nonholonomic left-invariant dynamics on Lie groups. The theory is illustrated with the discrete versions of two classical nonholonomic systems, the Suslov top and the Chaplygin sleigh. The preservation of the reduced energy by the discrete flow is observed and the discrete momentum conservation is discussed.

Contents

*AMS Subject Classification 37J60, 37J35, 70H45

1 Introduction

The theory of variational integrators for Lagrangian and Hamiltonian systems originated in [22], [23], and [18]. It was further developed by a number of authors (see e.g. [4], [14] [15], [24], and [17] for a more complete list of references and history). A very important feature of variational integrators is the *discrete momentum preservation*: if the original continuous-time system has a symmetry and conserves the momentum map, so does the associated discrete-time mechanical system.

In [6], [13] the theory was extended to the Lagrangian systems with nonholonomic constraints. In particular, it was shown in [6] that the discrete-time nonholonomic system conserves the *spatial* momentum in the case of *horizontal symmetry* (see [3] for the definition of the horizontal symmetry). However, the case of horizontal symmetry is not typical in nonholonomic mechanics. Apparently, Chaplygin [5] was the first to observe the link between symmetry and conservation of the components of momentum relative to the *moving* frame (see also [28] and references therein). Therefore, it is natural to ask whether the discrete momentum is preserved by the discrete-time nonholonomic system associated with a momentum-preserving continuous-time system. A closely related property is the existence of an invariant measure. The continuous-time nonholonomic systems generically are not measure-preserving (see [11] and [27] for details). The next version of this paper will address the measure-preservation property for the discrete-time nonholonomic systems.

The goal of this paper is to study the properties of the numerical variational integrators for a nonholonomic mechanical system whose configuration space is a Lie group G. Here we consider LL systems, that is, we assume that both the Lagrangian and the constraint distribution are invariant with respect to the induced left action of G on TG.

The paper is organized as follows: Section 2 gives a brief overview of both continuous and discrete-time nonholonomic systems.

In Section 3 we develop the theory of discrete left-invariant nonholonomic systems on Lie groups G. The fact that the constraints on $G \times G$ are left-invariant enables us to reduce the dynamics on a smooth *admissible displacement subvariety* $\mathcal{S} \subset G$, which is chosen to be the exponent of a linear subspace $\mathfrak{d}$ of the Lie algebra g of G. Under the discrete Legendre transformation, $\mathcal{S}$ gives rise to a discrete momentum locus $\mathcal{U}$ in the coalgebra g^*. In contrast to continuous nonholonomic systems, the locus is not a linear subspace in g^*, but rather a nonlinear subvariety. The dynamics is then described by the discrete Euler–Poincaré–Suslov equations that generate a (generally multivalued) map from $\mathcal{U}$ onto itself.

In Sections 4 and 5 we review the dynamics of the two classical nonholonomic LL systems on the Lie groups $SO(3)$ and $SE(2)$, the Suslov problem and the Chaplygin sleigh respectively, as well as their multidimensional generalizations.

In Sections 6 and 7 we construct the discretizations of the above problems as multi-valued maps on certain two-dimensional non-orientable subvarieties of $SO(3)$ and $SE(2)$. It is shown that the discrete model retains such a distinct feature of the continuous-time dynamics as the existence of heteroclinic trajectories that connect the two one-parameter families of relative equilibria of the system. If, for special values of parameters, the continuous-time system is momentum/measure preserving, then so is its discrete analog.

Moreover, it appears that in both discretizations the corresponding reduced constrained energy is preserved as well. This conservation law replaces the momentum conservation in the general case and seems to be quite unexpected, since generically the discrete variational integrators do not preserve the energy and this property does not change in the nonholonomic case.

2 Lagrangian Mechanics with Nonholonomic Constraints

In this section we briefly discuss the main concepts of nonholonomic dynamics. For a complete exposition see [2] and [3].

The Euler–Lagrange Equations for Nonholonomic Systems. A nonholonomic Lagrangian system is a triple $(Q, L, \mathcal{D})$, where Q is a smooth n-dimensional manifold called the *configuration space*, $L : TQ \to \mathbb{R}$ is a smooth function called the *Lagrangian*, and $\mathcal{D} \subset TQ$ is a k-dimensional *constraint distribution.* Let $q = (q^1, \ldots, q^n)$ be local coordinates on Q. In the induced coordinates $(q, \dot{q})$ on the tangent bundle TQ we write $L(q, \dot{q})$. It is assumed that the Lagrangian is *hyperregular*, *i.e.,* the map

$$\frac{\partial L}{\partial \dot{q}} : TQ \to T^*Q$$

is invertible (see [16]).

A curve $q(t) \in Q$ is said to *satisfy the constraints* if $\dot{q}(t) \in \mathcal{D}_{q(t)}$ for all t. The equations of motion are given by the following Lagrange–d'Alembert principle: *The Lagrange–d'Alembert equations of motion for the system are those determined by*

$$\delta \int_a^b L(q^i, \dot{q}^i)\, dt = 0, \tag{2.1}$$

where we choose variations $\delta q(t)$ *of the curve* $q(t)$ *that satisfy* $\delta q(a) = \delta q(b) = 0$ *and* $\delta q(t) \in \mathcal{D}_{q(t)}$ *for each* t *where* $a \le t \le b$. This principle is supplemented by the condition that the curve itself satisfies the constraints. Note that we take the variation *before* imposing the constraints; that is, we do not impose the constraints on the family of curves defining the variation. This is well known to be important to obtain the correct mechanical equations (see Bloch, Krishnaprasad, Marsden, and Murray [3] for a discussion and references).

Assuming that the constraint distribution is specified by a set of $n-k$ differential forms $A^j(q)$, $j = 1, \ldots, n-k$,

$$\mathcal{D} = \{\dot{q} \in TQ \mid \langle A^j(q), \dot{q} \rangle = 0,\ j = 1, \ldots, s = n-k\}, \tag{2.2}$$

equation (2.1) implies

$$\frac{d}{dt}\frac{\partial L}{\partial \dot{q}} - \frac{\partial L}{\partial q} = \sum_{j=1}^{s} \lambda_j A^j(q). \tag{2.3}$$

Equations (2.3) are called the *Euler–Lagrange equations with multipliers.* Coupled with (2.2), they give a complete description of the dynamics of the system.

Lemma 2.1. *Equations* (2.3) *conserve the energy*

$$E = \left\langle \frac{\partial L}{\partial \dot{q}}, \dot{q} \right\rangle - L. \tag{2.4}$$

Proof. Differentiating (2.4) along the flow (2.3), one obtains

$$\begin{aligned} \dot{E} &= \left\langle \frac{d}{dt}\frac{\partial L}{\partial \dot{q}}, \dot{q} \right\rangle + \left\langle \frac{\partial L}{\partial \dot{q}}, \ddot{q} \right\rangle - \left\langle \frac{\partial L}{\partial q}, \dot{q} \right\rangle - \left\langle \frac{\partial L}{\partial \dot{q}}, \ddot{q} \right\rangle \\ &= \left\langle \frac{d}{dt}\frac{\partial L}{\partial \dot{q}} - \frac{\partial L}{\partial q}, \dot{q} \right\rangle = \left\langle \sum_{j=1}^{s} \lambda_j A^j(q), \dot{q} \right\rangle = 0, \end{aligned}$$

since $\langle A^j(q), \dot{q} \rangle = 0$, $j = 1, \ldots, s$. □

The Euler–Poincaré–Suslov Equations. Let the configuration space be an n-dimensional connected Lie group G with local coordinates g. Let $\mathfrak{g}$ be the Lie algebra of G, that is, the tangent space T_eG at the identity element $e \in G$ supplied with an antisymmetric bracket operation $[\cdot\,,\cdot] : \mathfrak{g} \times \mathfrak{g} \to \mathfrak{g}$.

Define an *LL system* on G as a Lagrangian system $(G, L, \mathcal{D})$ with a left-invariant Lagrangian $L : TG \to \mathbb{R}$ and a left-invariant (generally nonintegrable) distribution $\mathcal{D}$ on the tangent bundle TG.

The Lagrangian $L : TG \to \mathbb{R}$ is left-invariant if and only if $L(g, \dot{g})$ depends on $(g, \dot{g})$ through the combination $\omega = g^{-1}\dot{g}$, *i.e.,* there exists a function $l : \mathfrak{g} \to \mathbb{R}$ called the *reduced Lagrangian* such that $L(g, \dot{g}) = l(\omega)$.

A distribution $\mathcal{D} \subset TG$ is left-invariant if and only if there is a subspace $\mathfrak{d} \subset \mathfrak{g}$ such that $\mathcal{D}_g = TL_g\, \mathfrak{d} \subset T_g G$ for any $g \in G$. Let $\mathfrak{g}^*$ be the dual of the Lie algebra and a^j, $j = 1, \dots, s$, be independent elements of $\mathfrak{g}^*$ associated with the subspace $\mathfrak{d}$, *i.e.,*

$$\mathfrak{d} = \{\xi \in \mathfrak{g} \mid \langle a^j, \xi\rangle = 0,\ j = 1, \dots, s\}.$$

Then the left-invariant constraints can be written as

$$\langle a^j, \omega\rangle = 0, \qquad j = 1, \dots, s, \tag{2.5}$$

where $\omega = g^{-1}\dot{g} = TL_{g^{-1}}\dot{g}$ is the *body velocity operator.*

Define the *body momentum* $p : \mathfrak{g}^* \to \mathbb{R}$ by the formula $p = \partial l/\partial\omega$. According to [12], the *reduced dynamics* of an LL system $(G, L, \mathcal{D})$ is governed by the *Euler–Poincaré–Suslov equations*

$$\dot{p} = \operatorname{ad}^*_\omega p + \sum_{j=1}^{s} \lambda^j a_j \tag{2.6}$$

coupled with the constraint equations (2.5). The dynamics of the group variables g is obtained by solving the *reconstruction equation*

$$\dot{g} = TL_g\, \omega. \tag{2.7}$$

Theorem 2.2. *The Euler–Poincaré–Suslov equations conserve the* ***reduced constrained energy***

$$\mathcal{E} = \left[\langle p, \omega\rangle - l(\omega)\right]_{\omega\in\mathfrak{d}}.$$

Proof. To prove this statement, observe that the reduced energy, $\langle p, \omega\rangle - l(\omega)$, equals the energy as the Lagrangian is left-invariant. Since $\omega \in \mathfrak{d}$ throughout the motion, the reduced constrained energy equals the energy along the trajectories of (2.6) and therefore is preserved. □

Let the reduced Lagrangian $l(\omega)$ be the quadratic form $l = \frac{1}{2}\langle\omega, \mathbb{I}\omega\rangle$, where $\mathbb{I} : \mathfrak{g} \to \mathfrak{g}^*$ is a symmetric non-singular *inertia operator.* In this case $p = \mathbb{I}\omega$. Then the constraints (2.5) imply that p lies in the subspace

$$\mathfrak{d}^\perp = \{\langle a^j, \mathbb{I}^{-1}p\rangle = 0,\ j = 1, \dots, s\} \subset \mathfrak{g}^*.$$

It is often convenient to choose a basis $e_1, \dots, e_n$ in the Lie algebra $\mathfrak{g}$ such that $a^j = e^{n-j+1}$, $j = 1, \dots, s$. In such a basis, the reduced constrained energy becomes

$$\frac{1}{2}\sum_{i,j=1}^{s} \mathbb{I}_{ij}\omega^i\omega^j = \frac{1}{2}\sum_{i,j=1}^{s} J^{ij} p_i p_j. \tag{2.8}$$

Here and elsewhere, the quantities J^{ij} represent the components of the *inverse constrained inertia operator* $\mathbb{I}_{|\mathfrak{d}}$.

Remark. In the absence of constraints, equations (2.6) become the Euler–Poincaré equations, which conserve the *spatial* momentum $J = \operatorname{Ad}^*_g p$. In the presence of nonholonomic constraints, neither the spatial, nor body momentum is conserved generically. However, in some cases the body momentum is preserved. (The conditions for the body momentum preservation can be seen in [28]).

Discrete Mechanical Systems with Nonholonomic Constraints. According to [6], a discrete nonholonomic mechanical system on Q is specified by

(i) a *discrete Lagrangian* $L_d : Q \times Q \to \mathbb{R}$;

(ii) an $(n-s)$-dimensional distribution $\mathcal{D}$ on TQ;

(iii) a discrete constraint manifold $\mathcal{D}_d \subset Q \times Q$, which has the same dimension as $\mathcal{D}$ and satisfies the condition $(q,q) \in \mathcal{D}_d$ for all $q \in Q$.

The dynamics is given by the following *discrete Lagrange–d'Alembert principle* (see [6]),

$$\sum_{k=0}^{N-1} \Big(D_1 L_d(q_k, q_{k+1}) + D_2 L_d(q_{k-1}, q_k) \Big) \delta q_k = 0, \quad \delta q_k \in \mathcal{D}_{q_k}, \quad (q_k, q_{k+1}) \in \mathcal{D}_d.$$

Here $D_1 L_d$ and $D_2 L_d$ denote the partial derivatives of the discrete Lagrangian with respect to the first and the second inputs, respectively.

The discrete constraint manifold is usually specified by the *discrete constraint functions*

$$\mathcal{F}_j(q_k, q_{k+1}) = 0, \qquad j = 1, \ldots, s, \tag{2.9}$$

which impose the restriction $(q_k, q_{k+1}) \in \mathcal{D}_d$ on the solution sequence $\{(q_k, q_{k+1})\}$.

Remark. If the discrete Lagrangian is obtained from a continuous one, $L(q, \dot{q})$, via a discretization mapping $\Psi : Q \times Q \to TQ$ defined in a neighborhood of the diagonal of $Q \times Q$, i.e., $L_d = L \circ \Psi$, then the variety $\mathcal{D}_d$ must be *consistent* with the continuous distribution $\mathcal{D}$: $\mathcal{D}_d$ is locally defined by the equations $\nu^j \circ \Psi = 0$, $j = 1, \ldots, s$. We emphasize that the discretization mapping is not unique and hence there are many ways to define the discrete Lagrangian L_d and the discrete constraint manifold $\mathcal{D}_d$ for a given nonholonomic system $(Q, L, \mathcal{D})$.[1]

The dynamics of a discrete nonholonomic system is represented by sequences $\{(q_k, q_{k+1})\}$ that satisfy the *discrete Lagrange–d'Alembert equations with multipliers*

$$D_1 L_d(q_k, q_{k+1}) + D_2 L_d(q_{k-1}, q_k) = \sum_{j=1}^{s} \lambda_j^k A^j(q_k), \quad \mathcal{F}_j(q_k, q_{k+1}) = 0. \tag{2.10}$$

As in the continuous-time case, these equations are equivalent the discrete Lagrange–d'Alembert principle.

Remark. According to [6], equations (2.10) introduce a well-defined mapping $(q_{k-1}, q_k) \mapsto (q_k, q_{k+1})$, if the $(n+s) \times (n+s)$ matrix

$$\begin{pmatrix} D_1 D_2 L_d(q_k, q_{k+1}) & A^1(q_k) & \cdots & A^s(q_k) \\ D_2 \mathcal{F}_1(q_k, q_{k+1}) & 0 & \cdots & 0 \\ \vdots & \vdots & & \vdots \\ D_2 \mathcal{F}_s(q_k, q_{k+1}) & 0 & \cdots & 0 \end{pmatrix}$$

is invertible for each (q_k, q_{k+1}) in a neighborhood of the diagonal of $Q \times Q$.

3 Discrete Euler–Poincaré–Suslov Equations

Continuous and Discrete Left-Invariant Lagrangians. Assume that the configuration space is a Lie group G and denote the local coordinates in G by g. Let the discrete Lagrangian $L_d : G \times G \to G$ be invariant with respect to the left diagonal action of G on $G \times G$:

$$L_d(g\, g_k, g\, g_{k+1}) = L_d(g_k, g_{k+1})$$

[1] An alternative approach to the discretization of nonholonomic systems based on a modification of canonical transformations was proposed in [13].

for any $g \in G$.

Define the *incremental displacement* by the formula $W_k = g_k^{-1} g_{k+1} \in G$. Since L_d is left-invariant, there exists a function $l_d : (G \times G)/G \cong G \to \mathbb{R}$ called the *reduced discrete Lagrangian* such that $L_d(g_k, g_{k+1}) = l_d(W_k)$.

According to [15], for a given continuous left-invariant Lagrangian $L(g, \dot g) = l(g^{-1}\dot g)$ its discrete analog l_d can be chosen in form

$$l_d = l((\log W_k)/h),$$

where $\log : G \to \mathfrak{g}$ is the (local) inverse of the exponential map $\exp : \mathfrak{g} \to G$ and $h \in \mathbb{R}_+$ is the given time step.

For a matrix group G, one can approximate $(\log W_k)/h$ with
$W_k - I \equiv g_k^{-1}(g_{k+1} - g_k)$, so that

$$L_d(g_k, g_{k+1}) = l\left(g_k^{-1}(g_{k+1} - g_k)/h\right). \tag{3.1}$$

This will be our default choice for the groups $SO(n)$ and $SE(n)$ considered in the next sections.

Similarly to [4, 15], we define the *discrete body momentum* $P_k : G \times G \to \mathfrak{g}^*$ by the formula

$$P_k = L^*_{g_k} D_2 L_d(g_{k-1}, g_k) \equiv L^*_{W_k} D\, l_d(W_k),$$

where $L^*_{g_k}$ is the induced left action $L^*_{g_k} : T^*G \to \mathfrak{g}^*$. Equivalently, P_k is defined by any of the conditions: for any $\omega \in \mathfrak{g}$, [2]

$$\langle \omega, P_k \rangle = -\frac{d}{d\varepsilon} L_d\left(g_k e^{\omega\varepsilon}, g_{k+1}\right)\bigg|_{\varepsilon=0} \quad \text{or} \quad \langle \omega, P_k \rangle = -\frac{d}{d\varepsilon} l_d\left(e^{\omega\varepsilon} W_k\right)\bigg|_{\varepsilon=0}. \tag{3.2}$$

In the unconstrained case, this defines the *discrete Legendre transformation* $\mathcal{L} : (g_k, W_k) \in G \times G \to (g_k, P_k) \in G \times \mathfrak{g}^*$. The mapping $\mathcal{L}$ is uniquely invertible in a neighborhood of the set $\{(g, P) \in G \times \mathfrak{g}^* \mid P = 0\}$, but it may fail to be globally invertible.

In the presence of generic discrete constraints (2.9), the displacement W_k is restricted to the *admissible displacement subvariety*

$$\mathcal{V}_k = \{W_k \in G \mid \mathcal{F}_j(g_k, g_k W_k) = 0,\ j = 1, \ldots, s\}$$

As a result, the discrete momentum P_k is restricted to an $(n-s)$-dimensional subvariety $\mathcal{U}_k \subset \mathfrak{g}^*$, the image of $\mathcal{L}(g_k, \mathcal{V}_k)$ in $\mathfrak{g}^*$. In case of generic discrete constraints, for different k the subvarieties $\mathcal{U}_k$ are different.

Discrete Left-Invariant Constraints. If the continuous constraint distribution $\mathcal{D}$ is left-invariant, it is natural to require that the discrete constraint manifold $\mathcal{D}_d$ is invariant with respect to the left diagonal action of G on $G \times G$, that is,

$$\mathcal{F}_j(g\, g_k, g\, g_{k+1}) = \mathcal{F}_j(q_k, q_{k+1}) \quad \text{for any} \quad g \in G, \quad j = 1, \ldots, s.$$

This implies that there exist functions $f_j : G \to \mathbb{R}$, $j = 1, \ldots, s$, such that

$$\mathcal{F}_j(q_k, q_{k+1}) = f_j(W_k).$$

Consequently, $\mathcal{D}_d \subset G \times G$ is completely defined by the admissible displacement subvariety

$$\mathcal{S} = \{f_1(W) = 0,\ \ldots,\ f_s(W) = 0\} \subset G,$$

[2] The definition of the discrete momentum (3.2) accepted in this paper computes p_k as a function of W_k whereas the standard definition used in many publications,

$$\langle \omega, P_k \rangle = \frac{d}{d\varepsilon} L_d\left(g_{k-1}, g_k e^{\omega\varepsilon}\right)\bigg|_{\varepsilon=0}.$$

makes p_k a function of W_{k-1}.

namely $\mathcal{D}_d = \{g, gh\}$, $g \in G, h \in \mathcal{S}$.

The submanifold $\mathcal{S}$ should pass through the identity element I in G, and the tangent space $T\mathcal{S}_I$ at the identity should be "horizontal", *i.e.,* it should coincide with the linear subspace $\mathfrak{d} \subset \mathfrak{g}$ generating the left-invariant distribution on TG.

The second property suggests that $\mathcal{S} = \{W \in G \mid \log W \in \mathfrak{d}\}$.

Equivalently, $\mathcal{S}$ can be chosen a union of all one-parameter subgroups G_ω generated by all admissible vectors $\hat{\omega} \in \mathfrak{d}$. In other words, one can set $\mathcal{S} = \exp \mathfrak{d}$. However, in case of generic $\mathfrak{d}$, the set $\exp \mathfrak{d}$ is not a subvariety of G.

In this paper we concentrate on the important case when G contains a subgroup H generated by subalgebra $\mathfrak{h} \subset \mathfrak{g}$ such that there is a decomposition $\mathfrak{g} = \mathfrak{h} \oplus \mathfrak{d}$ and $(\mathfrak{g}, \mathfrak{h})$ forms a symmetric pair, that is

$$[\mathfrak{h}, \mathfrak{h}] \subset \mathfrak{h}, \quad [\mathfrak{d}, \mathfrak{d}] \subset \mathfrak{h}, \quad [\mathfrak{h}, \mathfrak{d}] \subset \mathfrak{d}. \tag{3.3}$$

Proposition 3.1. ([10]) *Under the condition (3.3) the set $\mathcal{S} = \exp \mathfrak{d}$ is a smooth submanifold of G, which is either homeomorphic to the symmetric space G/H or is a factor of G/H by a finite group action.*

Under conditions (3.3) the set $\exp \mathfrak{d}$ is known as the Cartan model of the symmetric space G/H.

Notice that the tangent bundle $T\,S$ is not a subset of the left-invariant distribution $D \subset TG$, since the latter is not integrable.

Under the Legendre transformation $\mathcal{L}$, the discrete momentum P_k is confined to the subvariety

$$\mathcal{U} = \{p \in \mathfrak{g}^* \mid p = L_W^* l_d'(W), W \in \mathcal{S}\} \subset g^*,$$

which now does not depend on k. It appears that in the examples considered below the map $\mathcal{S} \mapsto \mathcal{U}$ is uniquely invertible almost everywhere on $\mathcal{U}$.

Discrete Euler–Poincerḗ–Suslov Equations. Assume that the discrete Lagrangian $L_d : G \times G \to \mathbb{R}$, the discrete constraint distribution $\mathcal{D}_d$, and the constraint distribution $\mathcal{D}$ are left-invariant with respect to the left action of G on $G \times G$ and TG, respectively.

Define the *action sum* and the *reduced action sum* by the formulae

$$S_d = \sum_{k=0}^{N-1} L_d(g_k, g_{k+1}) \quad \text{and} \quad s_d = \sum_{k=0}^{N-1} l_d(W_k),$$

respectively and rewrite the nonholonomic constraints (2.2) as a set of vanishing one-forms $A^j(g)\dot{g} = 0$.

Following [6], consider variation of S_d assuming that the variations δg_k satisfy the conditions $A^j(g_k)\delta g_k = 0$, $j = 1, \ldots, s$ and $\delta g_0 = \delta g_N = 0$.

For the left-invariant constraints given by (2.5) the admissible discrete variations are those $\delta g_k \in TG_{g_k}$ that satisfy the conditions

$$\langle a^j, g_k^{-1}\delta g_k\rangle = 0, \qquad j = 1, \ldots, s, \qquad k = 1, \ldots, N-1. \tag{3.4}$$

The following theorem extends the result of [4, 15] to the nonholonomic setting.

Theorem 3.2. *Let $L_d : G \times G \to \mathbb{R}$ be a left-invariant Lagrangian, $l_d : G \to \mathbb{R}$ be the reduced Lagrangian, and $\mathcal{D}$ and $\mathcal{D}_d$ be the compatible constraint distributions on TQ and $Q \times Q$, respectively. Then, following statements are equivalent:*

(i) The sequence $\{(g_k, g_{k+1})\}_{k=0}^{N-1}$ is a critical point of the action sum $S_d : G^{N+1} \to \mathbb{R}$ for arbitrary constrained variations.

(ii) The sequence $\{(g_k, g_{k+1})\}_{k=0}^{N-1}$ satisfies the discrete Euler–Lagrange equations with multipliers (2.10) with q replaced by g, that is,

$$D_1 L_d(g_k, g_{k+1}) + D_2 L_d(g_{k-1}, g_k) = \sum_{j=1}^{s} \lambda_k^j A_j(g_k) \tag{3.5}$$

which are coupled with the discrete constraint equations $\mathcal{F}_j(g_k, g_{k+1}) = 0$.

(iii) The sequence $\{W_k\}_{k=0}^{N-1}$ *is a critical point of the reduced action sum* $s_d : G^{N-1} \to \mathbb{R}$ *with respect to variations* δW_k*, induced by the constrained variations* δg_k*, and given by*

$$\delta W_k = W_k \left[g_{k+1}^{-1} \delta g_{k+1} - \mathrm{Ad}_{W_k^{-1}} \, g_k^{-1} \delta g_k \right]. \tag{3.6}$$

(iv) The sequence $\{W_k\}_{k=0}^{N-1}$ *satisfies the equations*

$$l'_d(W_{k-1}) TL_{W_{k-1}} - l'_d(W_k) TL_{W_k} \mathrm{Ad}_{W_k^{-1}} = \sum_{j=1}^{s} \lambda_k^j a_j \tag{3.7}$$

coupled with the discrete constraint equations

$$f_j(W_k) = 0, \qquad j = 1, \ldots, s, \quad k = 1, \ldots, N-1.$$

Proof of the theorem is given in the end of the section.

We now rewrite (3.7) in the form of discrete momentum equations. For any $\omega \in \mathfrak{g}$,

$$l'_d(W_{k-1}) TL_{W_{k-1}} \omega = \langle l'_d(W_{k-1}), TL_{W_{k-1}} \omega \rangle = \langle TL^*_{W_{k-1}} l'_d(W_{k-1}), \omega \rangle$$

and similarly

$$l'_d(W_k) TL_{W_k} \mathrm{Ad}_{W_k^{-1}} \omega = \langle l'_d(W_k), TL_{W_k} \mathrm{Ad}_{W_k} \omega \rangle = \langle \mathrm{Ad}^*_{W_k^{-1}} TL^*_{W_k} l'_d(W_k), \omega \rangle.$$

Therefore, in view of the definition of the discrete momentum (3.2), (3.7) becomes ***discrete Euler–Poincaré–Suslov equations***

$$P_{k+1} - \mathrm{Ad}^*_{W_k} P_k = \sum_{j=1}^{s} \lambda_{k+1}^j a_j, \tag{3.8}$$

where W_k is restricted to $\mathcal{S}$ and $p_k \in \mathcal{U} \subset \mathfrak{g}^*$.

The above equations extend the discrete Euler–Poincaré equations obtained in [4, 15] to the case when the discrete left-invariant constraints are present. Thus, they represent a discrete analog of (2.6) and define a map $\mathcal{B} : \mathcal{U} \mapsto \mathcal{U} : P_k \to P_{k+1}$, which is generally multi-valued. Given P_k, one evaluates P_{k+1} by

1. Finding W_k by inverting the Legendre transformation;
2. Calculating $\hat{P}_k = \mathrm{Ad}^*_{W_k} P_k$;
3. Choosing P_{k+1} as one of the points of intersection of the $(n-s)$-dimensional subvariety $\mathcal{U}$ with the linear space $\mathrm{span}(a_1, \ldots, a_s)$ passing through $\hat{P}_k$.

If the map is multivalued, one needs to make a choice of a branch of $\mathcal{B}$. One natural way of doing this is to start from a value of P_k whose norm is small and to select P_{k+1} of the smallest norm.

Proof of Theorem 3.2. We first prove the equivalence of (i) and (ii) following [6]. Recall that the variations δg_k vanish at $k = 0$ and $k = N$. Computing the first variation of the discrete action sum S_d, we obtain

$$\begin{aligned} \delta S_d &= \delta \sum_{k=0}^{N-1} L_d(g_k, g_{k+1}) \\ &= \sum_{k=0}^{N-1} D_1 L_d(g_k, g_{k+1}) \delta g_k + \sum_{k=0}^{N-1} D_2 L_d(g_k, g_{k+1}) \delta g_{k+1} \\ &= \sum_{k=1}^{N-1} D_1 L_d(g_k, g_{k+1}) \delta g_k + \sum_{k=1}^{N-1} D_2 L_d(g_{k-1}, g_k) \delta g_k \\ &= \sum_{k=1}^{N-1} \left(D_1 L_d(g_k, g_{k+1}) + D_2 L_d(g_{k-1}, g_k) \right) \delta g_k \,. \end{aligned}$$

Here the variations δg_k are not independent and satisfy the conditions $A_j(g_k)\delta g_k = 0$. Therefore, $\delta S_d = 0$ if and only if (3.5) is fulfilled.

Next, we prove that (i) is equivalent to (iii). Notice that $L_d = l_d \circ \pi$, where $\pi : G \times G \to (G \times G)/G \cong G$ is given by $(g_k, g_{k+1}) \mapsto g_k^{-1} g_{k+1}$. Therefore

$$\delta s_d = \delta S_d.$$

The variation δW_k is computed to be

$$\begin{aligned}
\delta W_k &= \delta(g_k^{-1} g_{k+1}) = g_k^{-1}\delta g_{k+1} + \delta g_k^{-1} g_{k+1} \\
&= g_k^{-1}\delta g_{k+1} - g_k^{-1}\delta g_k g_k^{-1} g_{k+1} \\
&= (g_k^{-1} g_{k+1})(g_{k+1}^{-1}\delta g_{k+1}) - (g_k^{-1} g_{k+1})(g_k^{-1} g_{k+1})^{-1}(g_k^{-1}\delta g_k)(g_k^{-1} g_{k+1}) \\
&= g_k^{-1} g_{k+1}\left[g_{k+1}^{-1}\delta g_{k+1} - \mathrm{Ad}_{\left(g_k^{-1} g_{k+1}\right)^{-1}}\left(g_k^{-1}\delta g_k\right)\right],
\end{aligned}$$

which yields (3.6).

To prove the equivalence of (iii) and (iv), we use (3.6) to compute

$$\begin{aligned}
\delta s_d &= \delta \sum_{k=0}^{N-1} l_d(W_k) = \sum_{k=0}^{N-1} \delta l_d(W_k) = \sum_{k=0}^{N-1} l_d'(W_k)\delta W_k \\
&= \sum_{k=0}^{N-1} l_d'(g_k^{-1} g_{k+1}) g_k^{-1} g_{k+1}\left[g_{k+1}^{-1}\delta g_{k+1} - \mathrm{Ad}_{\left(g_k^{-1} g_{k+1}\right)^{-1}}\left(g_k^{-1}\delta g_k\right)\right] \\
&= \sum_{k=1}^{N} l_d'\left(g_{k-1}^{-1} g_k\right)\left(g_{k-1}^{-1} g_k\right)\left(g_k^{-1}\delta g_k\right) \\
&\qquad - \sum_{k=0}^{N-1} l_d'\left(g_k^{-1} g_{k+1}\right)\left(\left(g_k^{-1} g_{k+1}\right)\mathrm{Ad}_{\left(g_k^{-1} g_{k+1}\right)^{-1}}\left(g_k^{-1}\delta g_k\right)\right) \\
&= \sum_{k=1}^{N-1}\Big[l_d'\left(g_{k-1}^{-1} g_k\right) TL_{g_{k-1}^{-1} g_k} \\
&\qquad - l_d'\left(g_k^{-1} g_{k+1}\right) TL_{g_k^{-1} g_{k+1}}\mathrm{Ad}_{\left(g_k^{-1} g_{k+1}\right)^{-1}}\Big]\left(g_k^{-1}\delta g_k\right).
\end{aligned}$$

Since the variations δg_k satisfy the conditions (3.4), $\delta s_d = 0$ if and only if item (iv) holds.

4 The Suslov Problem and its Multidimensional Generalizations

The most natural example of LL systems is the nonholonomic Suslov problem, which describes the motion of a rigid body about a fixed point under the action of the following nonholonomic constraint: the projection of the angular velocity vector $\overrightarrow{\omega} \in \mathbb{R}^3$ to a certain *fixed in the body* unit vector $\overrightarrow{\gamma}$ equals zero:

$$(\overrightarrow{\omega}, \overrightarrow{\gamma}) = 0. \tag{4.1}$$

The configuration space of the problem is the group $SO(3)$. Under the identification of Lie algebras $(\mathbb{R}^3, \times)$ and $(so(3), [\cdot,\cdot])$, $\overrightarrow{\omega}$ and $\overrightarrow{\gamma}$ correspond to elements of $so(3)$ and the coalgebra $so^*(3)$ respectively.

Let $\mathbb{I} : \mathbb{R}^3 \mapsto \mathbb{R}^3$ be the inertia tensor of the body. Then the Lagrangian equals $L = \frac{1}{2}(\overrightarrow{\omega}, \mathbb{I}\overrightarrow{\omega})$ and the momentum p is represented by the vector $\overrightarrow{M} = (M_1, M_2, M_3)^T = \mathbb{I}\overrightarrow{\omega}$. The left action of the group $SO(3)$ on $TSO(3)$ leaves the kinetic energy of the body and the constraint (4.1) invariant.

For the Suslov problem the Euler–Poincaré–Suslov equations (2.6) on $so(3)$ become

$$\frac{d}{dt}(\mathbb{I}\overrightarrow{\omega}) = \mathbb{I}\overrightarrow{\omega} \times \overrightarrow{\omega} + \lambda\overrightarrow{\gamma}, \tag{4.2}$$

where $\times$ denotes the vector product in $\mathbb{R}^3$ and λ is the Lagrange multiplier. Differentiating (4.1), we find

$$\lambda = -(\mathbb{I}\overrightarrow{\omega} \times \overrightarrow{\omega}, \mathbb{I}^{-1}\gamma)/(\overrightarrow{\gamma}, \mathbb{I}^{-1}\overrightarrow{\gamma}).$$

Therefore, (4.2) can be represented as

$$\frac{d}{dt}(\mathbb{I}\overrightarrow{\omega}) = \frac{1}{(\gamma, \mathbb{I}^{-1}\overrightarrow{\gamma})}\mathbb{I}^{-1}\overrightarrow{\gamma} \times ((\mathbb{I}\overrightarrow{\omega} \times \overrightarrow{\omega}) \times \overrightarrow{\gamma}),$$

which, in view of (4.1), is equivalent to

$$\frac{d}{dt}(\mathbb{I}\overrightarrow{\omega}) = (\mathbb{I}\overrightarrow{\omega}, \overrightarrow{\gamma})\, \overrightarrow{\omega} \times \mathbb{I}^{-1}\overrightarrow{\gamma}. \tag{4.3}$$

The Suslov system possesses the energy integral

$$(\overrightarrow{\omega}, \mathbb{I}\overrightarrow{\omega}) \equiv (\overrightarrow{M}, \mathbb{I}^{-1}\overrightarrow{M}) = h, \qquad h = \text{const} \tag{4.4}$$

and, as seen from (4.3), it has a line of equilibria positions

$$E = \{(\overrightarrow{\omega}, \overrightarrow{\gamma}) = 0\} \cap \{(\mathbb{I}\overrightarrow{\omega}, \overrightarrow{\gamma}) = 0\}.$$

Note that in the principal basis, where $\mathbb{I} = \text{diag}\,(\mathbb{I}_1, \mathbb{I}_2, \mathbb{I}_3)$, the system has the integral given by degenerate quadratic form

$$(\overrightarrow{M}, \hat{\mathbb{I}}\overrightarrow{M}), \quad \hat{\mathbb{I}} = \begin{pmatrix} \mathbb{I}_2\gamma_3^2 + \mathbb{I}_3\gamma_2^2 & -\mathbb{I}_3\gamma_1\gamma_2 & -\mathbb{I}_2\gamma_1\gamma_3 \\ -\mathbb{I}_3\gamma_1\gamma_2 & \mathbb{I}_1\gamma_3^2 + \mathbb{I}_3\gamma_1^2 & -\mathbb{I}_1\gamma_2\gamma_3 \\ -\mathbb{I}_2\gamma_1\gamma_3 & -\mathbb{I}_1\gamma_2\gamma_3 & \mathbb{I}_1\gamma_2^2 + \mathbb{I}_2\gamma_1^2 \end{pmatrix}, \tag{4.5}$$

which coincides with the restriction of (4.4) onto the constraint plane $(\overrightarrow{M}, \mathbb{I}^{-1}\overrightarrow{\gamma}) = 0$.

In the basis where only one of the components of $\overrightarrow{\gamma}$ is nonzero, say $\overrightarrow{\gamma} = (0, 0, 1)^T$, and the inertia tensor is unbalanced, the integral (4.4) can be replaced by the reduced constrained energy integral

$$\mathbb{I}_{22}M_1^2 - 2\mathbb{I}_{12}M_1M_2 + \mathbb{I}_{11}M_2^2. \tag{4.6}$$

The dynamics of the two independent momentum components, M_1 and M_2, is illustrated in the Figure 4.1. Because of the conservation law (4.6), the trajectories are the elliptic arches that form the heteroclinic connections between the asymptotically stable (filled dots) and unstable (empty dots) equilibria.

As a result, the motion of the rigid body is the asymptotic evolution from a permanent rotation about an axis fixed in the body frame to a permanent rotation about the same axis and with the same angular velocity, but in the opposite direction. Note that *in space* the axes of the limit permanent rotations are different.

The Suslov problem admits some natural multidimensional generalizations studied in [7, 9, 26]. The configuration space of an n-dimensional rigid body with a fixed point is the Lie group $SO(n)$. For a path $R(t) \in SO(n)$, the angular velocity of the body is defined as the left-trivialization $\omega(t) = g^{-1} \cdot g(t) \in so(n)$.

The left-invariant metric on $SO(n)$ is given by non-degenerate inertia operator $\mathbb{I} : so(n) \to so(n)$. Then the Lagrangian of the free motion of the body reads

$$L = \frac{1}{2}\langle \mathbb{I}\omega, \omega \rangle, \tag{4.7}$$

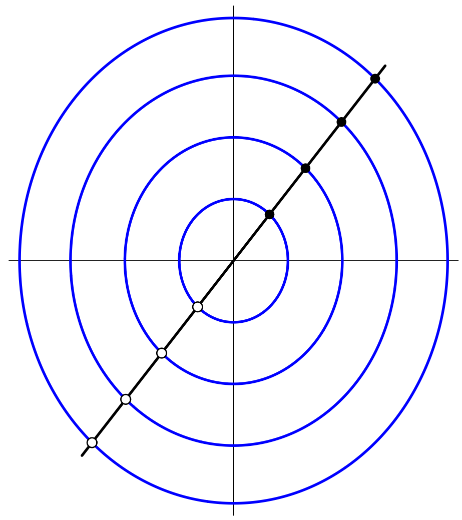

Figure 4.1: The Momentum Dynamics for the Suslov Problem.

where now $\langle \cdot, \cdot \rangle$ denotes the Killing metric on $so(n)$, $\langle X, Y \rangle = -\frac{1}{2}\text{tr}\,(XY)$, $X, Y \in so(n)$. For a "physical" rigid body, $\mathcal{I}\omega$ has the form $J\omega + \omega J$, where J is a symmetric $n \times n$ matrix called *mass tensor* (see [7]).

Let $e_1, \dots, e_n$ be the orthogonal frame of unit vectors fixed in the body. What form may have a multi-dimensional analog of the condition (4.1)? To answer this question, note that, instead of rotations *about an axis* in the classical mechanics, in the n-dimensional case we have infinitesimal rotations in the two-dimensional planes spanned by the basis vectors e_i, e_j, $i, j = 1, \dots, n$.

Suppose, without loss of generality, that $\overrightarrow{\gamma} = (0, 0, 1)$ in (4.1). Then this condition can be redefined as follows: only infinitesimal rotations in planes (e_1, e_3) and (e_2, e_3) are allowed. Hence, it is natural to define the n-dimensional analog of Suslov's condition in the following way: only infinitesimal rotations in the planes $(e_1, e_n), \dots, (e_{n-1}, e_n)$ (i.e., in the planes containing the vector e_n) are allowed. Thus, in the above basis, the angular velocity matrix in the body must have the form

$$\omega = \begin{pmatrix} 0 & \dots & 0 & \omega_{1n} \\ \vdots & & & \vdots \\ 0 & & & \omega_{n-1,n} \\ -\omega_{1n} & \dots & -\omega_{n-1,n} & 0 \end{pmatrix}. \tag{4.8}$$

This implies the constraints

$$\langle \omega, e_i \wedge e_j \rangle \equiv (e_i, \omega e_j) = 0, \quad 1 \le i < j \le n-1. \tag{4.9}$$

As a result, the multidimensional Suslov problem is described by the EPS equations on the Lie algebra $so(n)$

$$\frac{d}{dt}(\mathbb{I}\omega) = [\mathcal{I}\omega, \omega] + \sum_{1<p<q\le n-1} \lambda_{pq}\, e_p \wedge e_q, \tag{4.10}$$

where the multipliers λ_{pq} can be found by differentiating the constraints (4.9).

Integrability of the system (4.10), (4.9) was proved, and its geometric properties were studied in [7], whereas the reconstructed motion on the group $SO(n)$ was described in [26].

5 Chaplygin Sleigh

Another example of a mechanical system governed by the Euler–Poincaré–Suslov equations is the so-called Chaplygin sleigh, the system introduced and studied in 1911 by Chaplygin [5] (the work had been actually finished in 1906, see also [19]).

The sleigh is a rigid body moving on a horizontal plane supported at three points, two of which slide freely without friction while the third is a knife edge which allows no motion orthogonal to its direction, as shown in Figure 5.1.

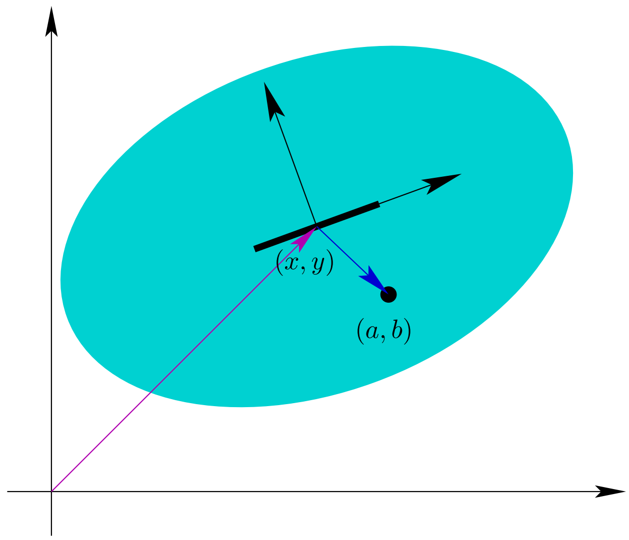

Figure 5.1: The Chaplygin Sleigh

The configuration space of this dynamical system is the group of Euclidean motions of the two-dimensional plane $\mathbb{R}^2$, $SE(2)$, which we parameterize with coordinates (θ, x, y). As the figure indicates, θ and (x, y) are the angular orientation of the blade and position of the contact point of the blade on the plane, respectively.

The Lagrangian and Constraint in the Body Frame. Introduce a coordinate system called the *body frame* by placing the origin at the contact point and choosing the first coordinate axis in the direction of the knife edge. Denote the angular velocity of the body by $\omega = \dot{\theta}$, and the components of the linear velocity of the contact point relative to the body frame by v_1, v_2. The set (ω, v_1, v_2) is regarded as an element of the Lie algebra $se(2)$.

The position of the center of mass is specified by the coordinates (a, b) relative to the body frame (we not assume here that the center of mass lie along the blade direction as in some models). We will see that a is crucial to qualitative behavior of the system while b is irrelevant.

The Lagrangian equals the kinetic energy of the body, which is a sum of the kinetic energy of the center of mass and the kinetic energy due to the rotation of the body. Let m and J denote the mass and moment of inertia of the sleigh relative to the contact point. The position of the center of mass relative to the fixed (inertial) frame is

$$(x + a\cos\theta - b\sin\theta, y + a\sin\theta + b\cos\theta).$$

Thus, the kinetic energy of the center of mass has the form

$$m\left[\dot{x}^2 + \dot{y}^2 + (a^2 + b^2)\dot{\theta}^2 + 2\dot{\theta}\left(a(-\dot{x}\sin\theta + \dot{y}\cos\theta) - b(\dot{x}\cos\theta + \dot{y}\sin\theta)\right)\right],$$

or, using the body components of the angular and linear velocity,

$$m\left[(a^2 + b^2)\omega^2 + v_1^2 + v_2^2 - 2b\omega v_1^2 + 2a\omega v_2\right].$$

As a result, the (reduced) Lagrangian is

$$l = \frac{1}{2}\left[(J + m(a^2 + b^2))\omega^2 + m(v_1^2 + v_2^2) - 2mb\omega v_1^2 + 2ma\omega v_2\right]. \tag{5.1}$$

Next, the constraint written relative to the body frame is $v_2 = 0$. Both the Lagrangian and constraint are invariant with respect to the left action of $SE(2)$ on $TSE(2)$ as they depend on $(g, \dot{g})$ through the combination

$$\Omega = g^{-1}\dot{g}. \tag{5.2}$$

The Dynamics of Chaplygin Sleigh. In view of (5.1), the components of the body momentum are

$$p_\theta \equiv \frac{\partial l}{\partial \omega} = (J + m(a^2+b^2))\omega + 2m(av_2 - bv_1),$$
$$p_1 \equiv \frac{\partial l}{\partial v_1} = m(v_1 - b\omega), \quad p_2 \equiv \frac{\partial l}{\partial v_2} = m(v_2 + a\omega).$$

The reduced dynamics of the Chaplygin sleigh is governed by the equations

$$\dot{p}_\theta = p_1 v_2 - p_2 v_1, \quad \dot{p}_1 = p_2\omega, \quad \dot{p}_2 = -p_1\omega + \lambda, \tag{5.3}$$

which are the Euler–Poincaré–Suslov equations (2.6) on the algebra $se(2)$ coupled with the constraint $v_2 = 0$. Eliminating the variables Ω and the Lagrange multiplier λ from (5.3), one obtains the reduced dynamics of the Chaplygin sleigh in the form of the momentum equation

$$\begin{aligned} \dot{p}_\theta &= -\frac{a}{(J+ma^2)^2}\,(p_\theta + b\,p_1)\left(mb\,p_\theta + (J + m(a^2+b^2))\,p_1\right), \\ \dot{p}_1 &= \frac{ma}{(J+ma^2)^2}\,(p_\theta + b\,p_1)^2, \end{aligned} \tag{5.4}$$

which has the constrained energy integral

$$mp_\theta^2 + 2bmp_\theta p_1 + (J + m(a^2+b^2))p_1^2. \tag{5.5}$$

In the case $b = 0$ equations (5.4) become

$$\dot{p}_\theta = -\frac{a\,p_\theta p_1}{J+ma^2}, \qquad \dot{p}_1 = \frac{ma\,p_\theta^2}{(J+ma^2)^2}. \tag{5.6}$$

We emphasize that the phase portrait of (5.4) is identical to that in the Suslov problem. Indeed, if $a = 0$, the nonholonomic momentum (p_θ, p_1) is conserved. Therefore, the body angular velocity ω and the component of the body linear velocity along the blade v_1 are constants. The evolution of the configuration variables (θ, x, y) is determined from the *reconstruction equation* (5.2), which reads

$$\dot{\theta} = \omega, \qquad \dot{x}\cos\theta + \dot{y}\sin\theta = v_1, \qquad -\dot{x}\sin\theta + \dot{y}\cos\theta = 0. \tag{5.7}$$

The solutions of (5.7) are

$$\theta = \theta_0 + \omega t, \quad x = x_0 + \frac{v_1}{\omega}\sin(\theta_0 + \omega t), \quad y = y_0 - \frac{v_1}{\omega}\cos(\theta_0+\omega t) \quad \text{if} \quad \omega \neq 0$$

and

$$\theta = \theta_0, \quad x = x_0 + v_1\cos\theta_0\, t, \quad y = y_0 + v_1 \sin\theta_0 \quad \text{if} \quad \omega = 0.$$

Therefore, the contact point of the blade and the plane generically moves along a circle at a uniform rate.

If $a \neq 0$, the dynamics (5.4) is integrable as the reduced energy is conserved. The trajectories of (5.4) are either equilibria situated on the line $p_\theta + bp_1 = 0$, or elliptic arches.[3] The equilibria located in the upper half plane are asymptotically stable (filled dots in Figure 5.2) whereas the equilibria in the lower half plane are unstable (empty dots in Figure 5.2). The elliptic arches form heteroclinic connections between the pairs of equilibria as shown in Figure 5.2.

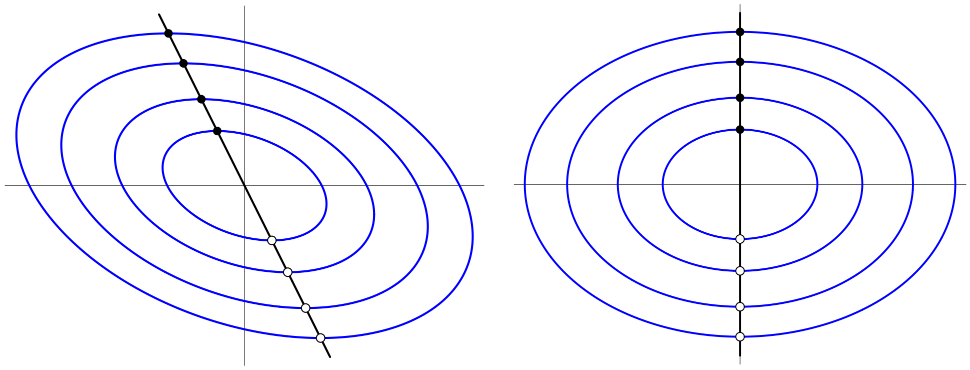

(a) $a \neq 0, b \neq 0$ (b) $a \neq 0, b = 0$

Figure 5.2: Momentum dynamics.

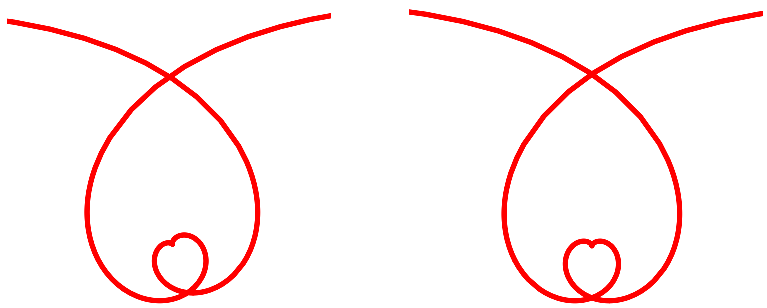

(a) $a \neq 0, b \neq 0$ (b) $a \neq 0, b = 0$

Figure 5.3: Generic trajectory of the blade.

A generic trajectory of the contact point of the blade and the plane has a cusp point (see Figure 5.3). At the cusp, the speed of the contact point, $|v_1|$, momentarily vanishes as the momentum trajectory intersects the line $mbp_1 + (J + m(a^2 + b^2))p_2 = 0$.

Since the group $SE(2)$ is a "non-compact" version of the group $SO(3)$, the dynamics of the Chaplygin sleigh can be interpreted as a "non-compact limit" of the dynamics of the Suslov problem. Recall that the any non-equilibrium trajectory of the Suslov top has a steady-state rotation as its asymptotic dynamics. In a similar manner, a non-equilibrium state of the Chaplygin sleigh asymptotically approaches a uniform straight-line motions as $t \to \pm\infty$.

The shape of the generic trajectory of the contact point is predetermined by the inertia of the body and the position of the center of mass relative to the blade, and is independent of the initial conditions. While the dynamics of the group variables (θ, x, y) cannot be explicitly written, it is possible to compute the angle between the asymptotic directions of the dynamics of the contact point. See [5] and [19] for details.

Multidimensional Chaplygin Sleigh. We now briefly discuss the generalized Chaplygin sleigh, which is an n-dimensional rigid body moving in $\mathbb{R}^n$ in the presence of certain

[3] This follows from matching the trajectories and the level curves of the reduced energy, which is a positive-definite quadratic form.

nonholonomic constraints.

The configuration space of this dynamical system is the group $SE(n)$, which has the structure of a semidirect product, $SE(n) = SO(n) \circledS \mathbb{R}^n$, so the group elements are written as (R, x), where $R \in SO(n)$ is the orthogonal rotation matrix of the body and $x \in \mathbb{R}^n$ is the position vector of its origin A. It is often convenient to represent the elements of $SE(n)$ by means of $(n+1) \times (n+1)$ matrices of the form

$$g(R, x) = \begin{pmatrix} R & x \\ 0 & 1 \end{pmatrix},$$

and the group operations for $SE(n)$ correspond to operations with the matrices: the product of two such matrices corresponds to the superposition of two Euclidean motions represented by these matrices and the inverse matrix correspond to the inverse Euclidean motion.

The Lie algebra $se(n)$ of the group $SE(n)$ is the semidirect product $so(n) \circledS \mathbb{R}^n$ and it is isomorphic to the set of $(n+1) \times (n+1)$ matrices

$$\eta = \begin{pmatrix} \xi & v \\ 0 & 0 \end{pmatrix}, \quad \xi \in so(n), \quad v \in \mathbb{R}^n.$$

The elements of $se(n)$ are written as (ξ, v). The Lie bracket $[\eta_1, \eta_2]$ in $se(n)$ is $\eta_1\eta_2 - \eta_2\eta_1$, which yields

$$[(\xi_1, v_1), (\xi_2, v_2)] = ([\xi_1, \xi_2], \xi_1 v_2 - \xi_2 v_1).$$

For a trajectory $g(t) \subset SE(n)$, the body velocity operator is defined as the left-trivialization $\xi(t) = g^{-1}\dot{g}(t) \in se(n)$. In this case $\omega = R^{-1}\dot{R}(t)$ and $v = R^{-1}\dot{x}(t)$ are respectively the angular velocity matrix and the vector of linear velocity of A in the body frame.

As in the classical case, we suppose that the center of mass $\mathbf{C}$ of the body does not coincide with the origin A of the body frame. Let $(a_1, \dots, a_n)^T$ be constant position vector of $\mathbf{C}$ in this frame and, as above, $J = \operatorname{diag}(J_1, \dots, J_n)$ be its mass tensor. Then the Lagrangian is

$$L = -\frac{1}{4}\operatorname{tr}\,(\xi\, \mathbb{J}\, \xi^T) \equiv -\frac{1}{4}\operatorname{tr}\,(\omega(J + ma \otimes a)\omega) + m(v, \omega a) + \frac{m}{2}(v, v), \tag{5.8}$$

$$\mathbb{J} = S \operatorname{diag}\,(J_1, \dots, J_n, m)\; S^T, \quad S = \begin{pmatrix} 1 & & & a_1 \\ & \ddots & & \vdots \\ & & 1 & a_n \\ 0 & \dots & 0 & 1 \end{pmatrix} \in SE(n),$$

where S describes the position of the center of mass $\mathbf{C}$ relative to the body frame.

The body momentum is an element of the dual space $se^*(n)$ and it is given by the pair

$$P = (M, p) \in se^*(n), \qquad M \in so(n), \quad p \in \mathbb{R}^n,$$
$$M_{ij} = \frac{\partial L}{\partial \omega_{ij}}, \quad p_i = \frac{\partial L}{\partial v_i}, \qquad i, j = 1, \dots, n.$$

Straightforward evaluation leads to the formulae

$$\begin{aligned} M &= (J + ma \otimes a)\omega + \omega(J + ma \otimes a) + m(v \otimes a - a \otimes v) \in so(n), \\ p &= m(v + \omega a) \in \mathbb{R}^n. \end{aligned} \tag{5.9}$$

Here M is the angular momentum of the body with respect to its center of mass C and p is the linear momentum of C as a point with mass m.

Left-invariant constraints on $SE(n)$. There are numerous ways to introduce nonholonomic constraints for the generalized Chaplygin sleigh. For example, one can require that the velocity of the reference point is restricted to a k-dimensional linear subspace fixed in the body. For $n = 3$, such constraints were studied in [19] and [27].)

Another natural choice is to define the constraint subspace $\mathfrak{d} \in se(n)$ to be the set of matrices of the form

$$\begin{pmatrix} 0 & \omega_{12} & \cdots & \omega_{1n} & v_1 \\ -\omega_{12} & 0 & & 0 & 0 \\ \vdots & & & & \vdots \\ -\omega_{1n} & 0 & & 0 & 0 \\ 0 & 0 & \dots & 0 & 0 \end{pmatrix}. \tag{5.10}$$

In the particular case $n = 2$ we have

$$S = \begin{pmatrix} 0 & -\omega & v_1 \\ \omega & 0 & 0 \\ 0 & 0 & 0 \end{pmatrix}. \tag{5.11}$$

6 Discrete Suslov System on $SO(n)$

Now we apply the the discrete Euler–Poincare– Suslov equations (3.8) to construct a discretization of the Suslov problem. Let $R_k \in SO(n)$ be the orthogonal rotation matrix describing the k-th position of n-dimensional top.

Introduce the *finite rotation matrix* $\Omega_k = R_k^T R_{k+1}$, analog of the angular velocity ω in the body. Note that in the continuous limit, when $R_{k+1} = R_k + \varepsilon \dot{R}$, $\varepsilon << 1$, one has

$$\Omega_k = \mathbf{I} + R^{-1}\dot{R} = \mathbf{I} + \varepsilon\omega, \tag{6.1}$$

Define the left-invariant discrete Lagrangian on $SO(n) \times SO(n)$ by substituting ω in (4.7) by $R_k^T(R_{k+1} - R_k) \equiv \Omega_k - \mathbf{I}$. Using the property $R_k^T R_k = \mathbf{I}$, we get

$$l_d(\Omega_k) = \frac{1}{2}\,\mathrm{tr}(\Omega_k J), \quad \text{and} \quad L_d(R_k, R_{k+1}) = \frac{1}{2}\,\mathrm{tr}(R_k J R_{k+1}^T).$$

Then, following the definition (3.2), the body angular momentum $M_k \in so^*(n)$ has the form

$$M_k = R_k^{-1} R_{k+1} J - J R_{k+1}^T R_k \equiv \Omega_k J - J\Omega_k^T, \tag{6.2}$$

which in the above limit transforms to $J\omega + \omega J$, the standard relation between the angular velocity and momentum. The expressions for L_d, M_k were originally introduced in [18].

Remark. In the classical case $n = 3$ one can parameterize R_k in terms of the Euler angles θ_k, ψ_k, ϕ_k, as coordinates on $SO(3)$ (see e.g., [25]),

$$\begin{pmatrix} \cos\phi_k\cos\psi_k - \cos\theta_k\sin\phi_k\sin\psi_k & -\cos\phi_k\sin\psi_k - \cos\theta_k\sin\phi_k\cos\psi_k & \sin\theta_k\sin\phi_k \\ \sin\phi_k\cos\psi_k + \cos\theta_k\cos\phi_k\sin\psi_k & -\sin\phi_k\sin\psi_k + \cos\theta_k\cos\phi_k\cos\psi_k & -\sin\theta_k\cos\phi_k \\ \sin\theta_k\sin\psi_k & \sin\theta_k\cos\psi_k & \cos\theta_k \end{pmatrix}$$

Substituting these ones and analogous expressions for R_{k+1} into the discrete Lagrangian $L_d(R_k, R_{k+1})$, we obtain

$$
\begin{aligned}
L_d = \frac{1}{2}\Big[& \cos\theta_k\, \cos\theta_{k+1}\,[1+\cos(\Delta\phi_k)\, \cos(\psi_k+\psi_{k+1})] \\
& + \cos(\psi_k+\psi_{k+1})\, \sin\theta_k\, \sin\theta_{k+1} + \cos(\Delta\phi_k)[\sin\theta_k\, \sin\theta_{k+1} \\
& - \cos(\psi_k+\psi_{k+1})] + \frac{1}{2}[\cos\theta_{k+1} - \cos\theta_k]\, \sin(\Delta\phi_k)\, \sin(\psi_k+\psi_{k+1})\Big] A_1 \\
& + \frac{1}{2}\Big[\cos\vartheta_k\, \cos\vartheta_{k+1} + \cos(\Delta\phi_k)\, \cos(\Delta\psi_k) - \cos\vartheta_k\, \cos\vartheta_{k+1}\, \cos(\Delta\phi_k)\, \cos(\Delta\psi_k) \\
& + \cos(\Delta\phi_k)\, \sin\vartheta_k\, \sin\vartheta_{k+1} - \cos(\Delta\psi_k)\, \sin\vartheta_k\, \sin\vartheta_{k+1} \\
& - \cos\vartheta_k\, \sin(\phi_k+\phi_{k+1})\, \sin(\Delta\psi_k) - \cos\vartheta_{k+1}\, \sin(\Delta\phi_k)\, \sin(\psi_k+\psi_{k+1})\Big] A_2 \\
& - \frac{1}{2}\Big[\cos(\Delta\phi_k)\, \cos(\Delta\psi_k) + \cos\theta_k\, \cos\theta_{k+1}\, \cos(\Delta\phi_k)\, \cos(\Delta\psi_k) \\
& - \cos\theta_k\, \cos\theta_{k+1} + \sin\theta_k\, \sin\theta_{k+1}(\cos(\Delta\psi_k) - \cos(\Delta\phi_k)) \\
& - (\cos\theta_k + \cos\theta_{k+1})\sin(\Delta\phi_k)\, \sin(\Delta\psi_k)\Big] A_3
\end{aligned} \tag{6.3}
$$

where $\Delta\theta_k = \theta_{k+1} - \theta_k$, $\Delta\phi_k = \phi_{k+1} - \phi_k$, $\Delta\psi_k = \psi_{k+1} - \psi_k$, and

$$
A_1 = J_2 + J_3, \quad A_2 = J_1 + J_3, \quad A_3 = J_1 + J_2
$$

are the principal moments of inertia of the rigid body.

In the continuous limit, setting in (6.3)

$$
\theta_{k+1} - \theta_k = \dot\theta\, \delta t, \quad \phi_{k+1} - \phi_k = \dot\phi\, \delta t, \quad \psi_{k+1} - \psi_k = \dot\psi\, \delta t, \qquad \delta t << 1 \tag{6.4}
$$

then expanding in δt and dividing by $(\delta t)^2$, up to an additive constant and terms of order δt, one obtains the well-known expression for the kinetic energy of the top (see, e.g., [25])

$$
\begin{aligned}
T = & \frac{1}{2}(\dot\phi\sin\theta\sin\psi + \dot\theta\cos\psi)^2 A_1 \\
& + \frac{1}{2}(\dot\phi\sin\theta\cos\psi - \dot\theta\sin\psi)^2 A_2 + \frac{1}{2}(\dot\psi + \dot\phi\cos\theta)^2 A_3,
\end{aligned} \tag{6.5}
$$

where the expressions in brackets represent components of the angular velocity vector in the frame attached to the body.

Notice that the discrete Lagrangian (6.3) does not coincide with the "straightforward" discretization of (6.5) obtained with a direct replacement of the angular velocities by the angular differences according to (6.4).

Discrete constraints on $SO(n)$. Following the approach described in Section 2, we impose discrete left-invariant constraints on $SO(n) \times SO(n)$ in the form of restrictions on finite rotations $\Omega_k \in SO(n)$. In accordance with the continuous constraints (4.9), we assume that admissible rotations must be exponents of the vectors of the linear space

$$
\mathfrak{d} = \operatorname{span}\{e_1 \wedge e_n,\ \ldots, e_{n-1} \wedge e_n\} \subset so(n).
$$

Lemma 6.1. *1). In the basis $e_1, \ldots, e_n$, the admissible rotation matrices have the structure*

$$
(\Omega_k)_{ij} = (\Omega_k)_{ji}, \quad (\Omega_k)_{in} = -(\Omega_k)_{ni}, \qquad 1 \le i, j \le n-1, \tag{6.6}
$$

that is, they are anti-symmetric in its last row and column and symmetric in the other part.

2). The admissible displacement subvariety $S = \exp \mathfrak{d}$ is homeomorphic to the projective space $\mathbb{P}^{n-1} = S^{n-1}/\mathbb{Z}^2$. In the same basis, the components of Ω_k are parameterized by points of the unit sphere $S^{n-1} = \{z_0^2 + z_1^2 + \cdots + z_{n-1}^2 = 1\}$ in the form [4]

$$(\Omega_k)_{ij} = \delta_{ij} - 2z_i z_j, \quad (\Omega_k)_{in} = -(\Omega_k)_{ni} = 2z_0 z_i, \quad (\Omega_k)_{nn} = 2z_0^2 - 1, \qquad (6.7)$$
$$1 \le i, j \le n-1.$$

Note that in the continuous limit described by (6.1), conditions (6.6) yield the constraints (4.8) on $so(n)$.

Proof of Lemma 6.1. 1). Any vector of $\mathfrak{d} \subset so(n)$ can be represented in the form $\theta \mathbf{u} \wedge e_n$, where θ is a nonzero constant and $\mathbf{u} = (u_1, \dots, u_{n-1}, 0)^T$ is a unit vector in $\mathbb{R}^{n-1} = \text{span}\,(e_1, \dots, e_{n-1})$. The odd powers of $\theta \mathbf{u} \wedge e_n$ are skew-symmetric and have zero left-upper $(n-1) \times (n-1)$ part, whereas the even powers are symmetric and have zero last row and last column. Hence, the exponent of $\theta \mathbf{u} \wedge e_n$ must be of the form (6.6).

2). The operator $\mathcal{R}_{\theta,u} = \exp(\theta \mathbf{u} \wedge e_n) \subset SO(n)$ describes rotation in the 2-plane spanned by $\mathbf{u}, e_n$ by the angle θ. Then we get

$$\begin{aligned}
&\mathcal{R}_{\theta,u}\, \mathbf{u} = \cos\theta \cdot \mathbf{u} - \sin\theta \cdot e_n, \\
&\mathcal{R}_{\theta,u}\, e_j = e_j - (e_j, \mathbf{u})\mathbf{u} + (e_j, \mathbf{u})(\cos\theta \cdot \mathbf{u} - \sin\theta \cdot e_n), \qquad 1 \le j \le n-1, \\
&\mathcal{R}_{\theta,u}\, e_n = \cos\theta \cdot e_n + \sin\theta \cdot \mathbf{u}\,.
\end{aligned}$$

The latter n vectors form columns of the matrix $\mathcal{R}_{\theta,u}$. Setting in the above formulas

$$z_i = \sin\theta/2\, u_i, \quad 1 \le i, j \le n-1, \quad z_0 = \cos\theta/2 \qquad (6.8)$$

and identifying $\mathcal{R}_{\theta,u}$ with Ω_k we arrive at expressions (6.7).

Since $\sin(\theta/2) = -\sin(2\pi - \theta)/2$ and $\cos(\theta/2) = -\cos(2\pi - \theta)/2$, from (6.8) we conclude that opposite points on S^{n-1} correspond to the same admissible rotation $\mathcal{R}_{\theta,u}$. Finally, there is a bijection between $S = \exp \mathfrak{d}$ and $\mathbb{P}^{n-1} = S^{n-1}/\mathbb{Z}^2$. The lemma is proved.

Note that (6.6) imply left-invariant constraints on $SO(n) \times SO(n)$ in the form

$$\text{tr}(R_k^T\, e_j \wedge e_n\, R_{k+1} - R_{k+1}^T\, e_j \wedge e_n\, R_k) = 0\,, \qquad j = 1, \dots, n-1.$$

Rotations about an axis. In the classical case $n = 3$ the conditions (6.6) say that Ω_k is a finite rotation about an axis lying in the plane (e_1, e_2), while expressions (6.7) imply that the rotation axis is directed along vector $\rho = (z_2, -z_1, 0)^T \in \mathbb{R}^3$.

Indeed, the group $SO(3)$ can be regarded as covered twice by the unit sphere $S^3 = \{q_0^2 + q_1^2 + q_2^2 + q_3^2 = 1\}$, where $q_0, \dots, q_3$ are the Euler–Rodriguez parameters such that any rotation matrix $W \in SO(3)$ can be represented in form (see, e.g., [25])

$$W = \begin{pmatrix} q_0^2 + q_1^2 - q_2^2 - q_3^2 & 2(q_1 q_2 + q_3 q_0) & -2(q_1 q_3 - q_2 q_0) \\ 2(q_1 q_2 - q_3 q_0) & q_0^2 + q_2^2 - q_1^2 - q_3^2 & -2(q_2 q_3 + q_0 q_1) \\ -2(q_1 q_3 + q_2 q_0) & -2(q_2 q_3 - q_0 q_1) & q_0^2 + q_3^2 - q_1^2 - q_2^2 \end{pmatrix}. \qquad (6.9)$$

The operator W describes a finite rotation in $\mathbb{R}^3$ about the vector $\mathbf{e} = (q_1, q_2, q_3)^T$ by the angle θ such that $q_0 = \cos\theta/2$.

Setting in (6.9) $(\Omega_k)_{12} = (\Omega_k)_{21}$ implies $q_3 = 0$, hence W is a rotation about an axis lying in the plane (e_1, e_2). In this case admissible operators $\Omega \in \mathcal{S} \subset SO(3)$ have the form

$$\Omega = \begin{pmatrix} 2(q_0^2 + q_1^2) - 1 & 2q_1 q_2 & 2q_0 q_2 \\ 2q_1 q_2 & 2(q_0^2 + q_2^2) - 1 & -2q_0 q_1 \\ -2q_0 q_2 & 2q_0 q_1 & 2q_0^2 - 1 \end{pmatrix}, \qquad (6.10)$$

[4]Here and below, to simplify notation, we omit the discrete time index k at the components of z.

which, under the substitution $q_1 = -z_2$, $q_2 = z_1$, $q_0 = z_0$, coincides with the parameterization (6.7). As a result, the variety of such matrices is the real projective plane $\mathbb{RP}^2 = S^2/\mathbb{Z}^2$.

We emphasize that, in general, the k-th position of the body $R_k = \Omega_{k-1} \cdots \Omega_0$ *is not* a rotation in the plane (e_1, e_2).

Discrete momentum locus $\mathcal{U} \subset so^*(3)$. In contrast to the continuous case, the discrete momentum M_k does not lie in a linear subspace in the coalgebra $so^*(3)$, but on a nonlinear algebraic variety $\mathcal{U} \subset so^*(3)$ defined by the relation (6.2) and the conditions (6.10).

If in the frame e_1, e_2, e_3 the tensor J is diagonal, $J = \operatorname{diag}(J_1, J_2, J_3)^T$, then the angular momentum vector $\overrightarrow{M} = (M_1 = -M_{23}, M_2 = M_{13}, M_3 = -M_{12})^T$ has the form

$$\overrightarrow{M} = 2((J_2 + J_3)q_0q_1, (J_1 + J_3)q_0q_2, (J_1 - J_2)q_1q_2)^T$$

(as above, to avoid tedious notation we omit the discrete time index at the components of q). Here and below, without loss of generality, we always assume $q_0 \geq 0$. As a result, $\mathcal{U}$ coincides with *the Steiner Roman surface* in $\mathbb{R}^3$ given by the quartic equation

$$\begin{aligned}\frac{J_1 - J_2}{(J_2 + J_3)(J_1 + J_3)} M_1^2 M_2^2 + \frac{J_1 + J_3}{(J_2 + J_3)(J_1 - J_2)} M_1^2 M_3^2 \\ + \frac{J_2 + J_3}{(J_1 + J_3)(J_1 - J_2)} M_2^2 M_3^2 - 2M_1M_2M_3 = 0 \end{aligned} \tag{6.11}$$

(see, e.g., [8, 20]).

In general case, when J is not diagonal in this frame, one has the parameterization

$$\overrightarrow{M} = 2 \begin{pmatrix} (J_{22} + J_{33})q_0q_1 - J_{12}q_0q_2 & -(J_{13}q_1 + J_{23}q_2)q_2 \\ (J_{11} + J_{33})q_0q_2 - J_{12}q_0q_1 & +(J_{13}q_1 + J_{23}q_2)q_1 \\ (J_{11} - J_{22})q_1q_2 - J_{12}(q_1^2 - q_2^2) & -(J_{13}q_1 + J_{23}q_2)q_0 \end{pmatrix}. \tag{6.12}$$

One can show that the components of $\overrightarrow{M}$ satisfy an algebraic equation of degree 4, which generalizes (6.11) and which we do not write here. The corresponding algebraic surface $\mathcal{U}$ in $\mathbb{R}^3 = (M_1, M_2, M_3)$ has pinch points and self-intersections. One can also show that if the quadratic form $(J_{22}+J_{33})q_1^2 - 2J_{12}q_1q_2 + (J_{33}+J_{11})q_2^2$ is positive-definite, then any pair (M_1, M_2) has at most two real inverse images on $\mathcal{U}$.

An example of such a surface for an unbalanced inertia tensor and its circular section for $0.4 \leq q_0 \leq 0.8$ are given in Figures 6.1, 6.2 respectively.

Discrete EPS equations on $so^*(3)$. In the considered case $G = SO(3)$, the discrete momentum equation with multipliers (3.8) takes the form

$$M_{k+1} = \Omega_k^T M_k \Omega_k + \lambda_k \begin{pmatrix} 0 & 1 & 0 \\ -1 & 0 & 0 \\ 0 & 0 & 0 \end{pmatrix}, \quad M_k = \Omega_k J - J\Omega_k^T, \tag{6.13}$$

where the components of Ω_k are subject to constraints (6.6).

This provides a discrete analog of the Suslov system (4.10) on $so^*(3)$ and defines a map $\mathcal{U} \to \mathcal{U}$ or, in view of expressions (6.10), (6.12), a map
$\mathcal{B} : \mathbb{R}P^2 \to \mathbb{R}P^2 : (q_1, q_2, q_0) \to (\tilde{q}_1, \tilde{q}_2, \tilde{q}_0)$, which is generally multi-valued.

To describe the latter map in details, we note that in (6.13)

$$\begin{aligned}\overrightarrow{\Omega_k^T M_k \Omega_k} &\equiv \overrightarrow{J\Omega_k - \Omega_k^T J} \equiv \Omega_k^T \overrightarrow{M_k} \\ &= 2 \begin{pmatrix} (J_{22} + J_{33})q_0q_1 - J_{12}q_0q_2 & +(J_{13}q_1 + J_{23}q_2)q_2 \\ (J_{11} + J_{33})q_0q_2 - J_{12}q_0q_1 & -(J_{13}q_1 + J_{23}q_2)q_1 \\ -(J_{11} - J_{22})q_1q_2 + J_{12}(q_1^2 - q_2^2) & -(J_{13}q_1 + J_{23}q_2)q_0 \end{pmatrix}, \end{aligned} \tag{6.14}$$

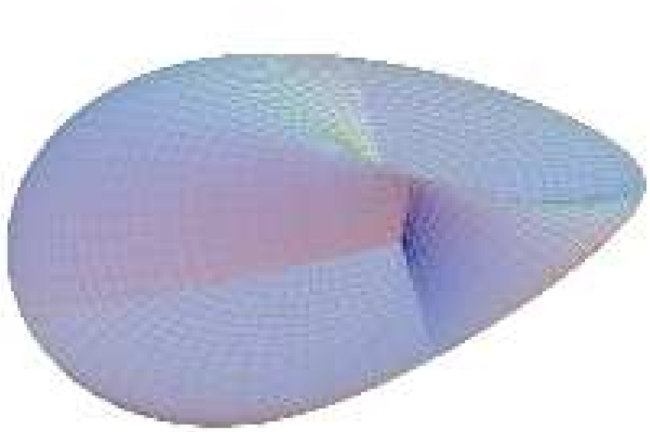

Figure 6.1: The Momentum Surface $\mathcal{U}$.

where $\overrightarrow{\omega}$ denotes vector representation of element ω of $so(3)$. Comparing this with (6.12), we find that (6.13) can be written in form

$$\overrightarrow{M_{k+1}} = \overrightarrow{M_k} + 4 \begin{pmatrix} (J_{13}q_1 + J_{23}q_2)q_2 \\ -(J_{13}q_1 + J_{23}q_2)q_1 \\ -(J_{11} - J_{22})q_1q_2 + J_{12}(q_1^2 - q_2^2) + \lambda_k \end{pmatrix}, \tag{6.15}$$

which can be viewed as a discrete analog of equations (4.3). This also shows that the difference vector $\overrightarrow{M_{k+1}} - \overrightarrow{M_k}$ is orthogonal to the rotation axis directed along $(q_1, q_2, 0) \in \mathbb{R}^3$, as expected.

As a result, the map $\mathcal{B} : \mathbb{RP}^2 \to \mathbb{RP}^2$ given by (6.13) consists of the following 3 steps:

1). Given original set $q_1, q_2, q_0 = \sqrt{1 - q_1^2 - q_2^2}$, one finds components of $\overrightarrow{M_k}$ from (6.12) and of $\overrightarrow{\Omega_k^T M_k \Omega_k}$ from (6.14).

2). Given the components

$$(\overrightarrow{M_{k+1}})_1 = (\overrightarrow{\Omega_k^T M_k \Omega_k})_1, \quad (\overrightarrow{M_{k+1}})_2 = (\overrightarrow{\Omega_k^T M_k \Omega_k})_2,$$

one finds new $\tilde{q}_1, \tilde{q}_2$ by solving the system of two algebraic equations originating from (6.12)

$$\begin{aligned} (\overrightarrow{M_{k+1}})_1 &= ((J_{22} + J_{33})\tilde{q}_1 - J_{12}\tilde{q}_2)\sqrt{1 - \tilde{q}_1^2 - \tilde{q}_2^2} - (J_{13}\tilde{q}_1 + J_{23}\tilde{q}_2)\tilde{q}_2, \\ (\overrightarrow{M_{k+1}})_2 &= ((J_{11} + J_{33})\tilde{q}_2 - J_{12}\tilde{q}_1)\sqrt{1 - \tilde{q}_1^2 - \tilde{q}_2^2} + (J_{13}\tilde{q}_1 + J_{23}\tilde{q}_2)\tilde{q}_1. \end{aligned} \tag{6.16}$$

In $\mathbb{R}^3 = (q_1, q_2, q_0)$ these equations describe two centrally symmetric quadratic surfaces Q_1, Q_2 which intersect the unit sphere $q_1^2 + q_2^2 + q_0^2 = 1$ along curves C_1, C_2 respectively. Each curve is a union of two ovals, which are centrally symmetric to each other. The intersection of C_1, C_2 gives 4 complex points and 2 or none real points on $\mathbb{P}^2$. Thus there are at most two different real solutions $(\tilde{q}_1^{(j)}, \tilde{q}_2^{(j)}, \tilde{q}_0^{(j)})$ with $\tilde{q}_0^{(j)} > 0$.

3). One chooses a solution $\left(\tilde{q}_1^{(1)}, \tilde{q}_2^{(1)}, \tilde{q}_0^{(1)} > 0\right)$ and finally finds the last component $(\bar{M}_{k+1})_3$ by the formula

$$(\bar{M}_{k+1})_3 = (J_{11} - J_{22})\tilde{q}_1\tilde{q}_2 - J_{12}(\tilde{q}_1^2 - \tilde{q}_2^2) - (J_{13}\tilde{q}_1 + J_{23}\tilde{q}_2)\tilde{q}_0,$$

which is obtained from (6.16) by substitutions $k \to k+1$ and the $q \to \tilde{q}$.

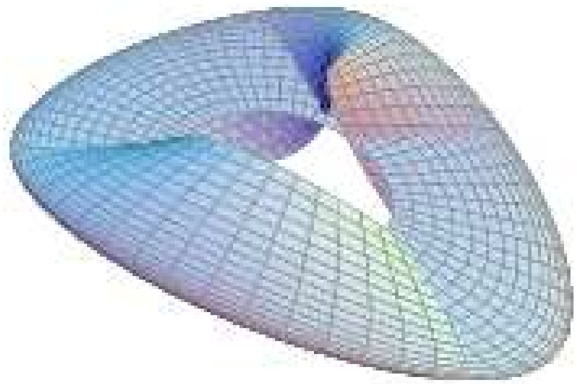

Figure 6.2: A Circular Section of the Momentum Surface

As a result, for $n = 3$ the map $M_k \to M_{k+1}$ given by (6.13) is generally *4-complex valued* and 2-real valued. In order to choose one of the 2 real branches, we must use some extra arguments, like existence of an additional integral, or, at least, to restrict ourselves with sufficiently small q_1, q_2, which correspond to rotations Ω by a small angle θ. In this case only one of the solutions $(\tilde{q}_1^{(j)}, \tilde{q}_2^{(j)})$ will be small and it is natural to choose it.

It appears that the constrained energy integral (4.6) of the continuous Suslov system is preserved by the discrete system as well.

Theorem 6.2. *The discrete Suslov system (6.13) has quadratic integral*

$$(J_{11} + J_{33})M_1^2 + 2J_{12}M_1M_2 + (J_{22} + J_{33})M_2^2, \tag{6.17}$$

which gives rise to the following quartic integral in terms of the parameters q_0, q_1, q_2*:*

$$\begin{aligned} H = &((J_{22} + J_{33})q_1^2 - 2J_{12}q_1q_2 + (J_{11} + J_{33})q_2^2) \\ &\cdot \left((J_{13}q_1 + J_{23}q_2)^2 + [(J_{11} + J_{33})(J_{22} + J_{33}) - J_{12}^2]q_0^2\right). \end{aligned} \tag{6.18}$$

The proof is straightforward: substituting expressions (6.12) and (6.14) into (6.17) gives the same expression in terms of q_0, q_1, q_2.

The fact that (6.17) does not depend on M_3 is quite natural: different branches of the map (6.13) have the same value of the integral.

It should be emphasized that the complete energy integral $(M, \mathbb{I}^{-1}M)$ of the continuous Suslov problem is not preserved in the discrete setting.

Invariant curves. As follows from Theorem 6.2, the map has invariant curves, which are either intersections of the sphere $\{q_1^2 + q_2^2 + q_0^2 = 1\}$ with a quartic surface $H(q) = h$ or, in the momentum space $so^*(3)$, intersections of the generalized quartic Steiner surface $\mathcal{U}$ with elliptic cylinders defined by (6.17). Thus, the invariant varieties are algebraic curves of order 8.

Assume that quadratic form $(J_{22} + J_{33})q_1^2 - 2J_{12}q_1q_2 + (J_{33} + J_{11})q_2^2$ is positive definite. Then, as follows from (6.18), on the upper hemisphere $0 \le q_0 \le 1$ real invariant curves consist of two branches: for small positive values of h one branch is a small oval around the origin $(0, 0)$ whereas the other branch is an oval close to the equator $\{q_0 = 0\}$ of the sphere. It may or may not intersect the equator. In the first case the opposite points of intersection are identified.

These different branches correspond to the two connected components of the intersection of the Steiner surface $\mathcal{U}$ with the cylinder.

As value of the integral increases, the branches approach each other: the smaller one becomes bigger and the bigger shrinks. At a certain critical value $h = h^*$ the branches intersect at two opposite saddle points and form a separatrix, and for the next critical value $h^{**} > h^*$ the two branches shrink to opposite center points. There are no real invariant curves for $h > h^{**}$. Note that for $h = h^*$ and $h = h^{**}$ the elliptic cylinder is tangent to the surface $\mathcal{U}$. An example of the invariant curves foliation is given in Figure 6.3.

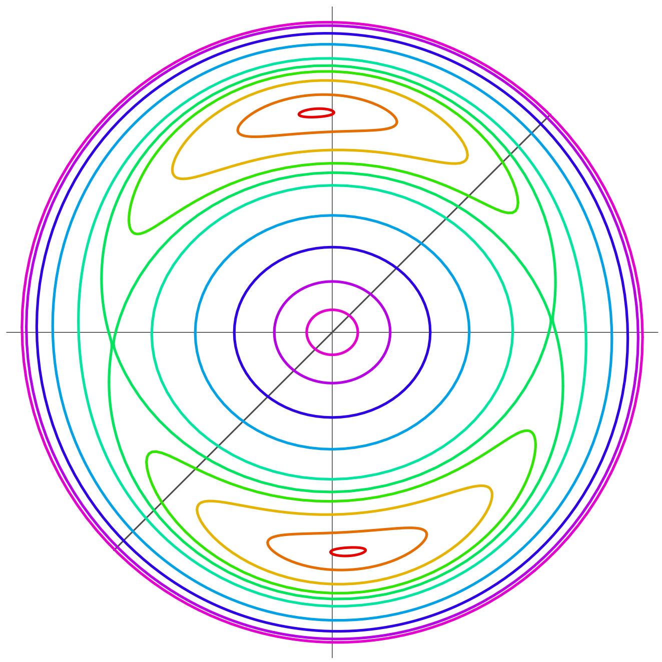

Figure 6.3: Invariant Curves and the Equilibria Line on $\mathbb{RP}^2$.

Remark. As noticed in [18], in the absence of nonholonomic constraints, the map $M_k \to M_{k+1}$ given by the discrete Euler–Poincaré equations (6.13) is multi-valued, because, in general, the equation $M_k = \Omega_k J - J\Omega_k^T$ has more than one solution.

In presence of the constraints (6.10), the latter equation has generally *a unique* solution (except the points on self-intersection on $\mathcal{U}$), however, as we saw above, the choice of λ_{k+1} or $(\bar{M}_{k+1})_3$ is not unique, and the map describing the discrete Suslov problem is multi-valued as well.

Stationary solutions of the discrete Suslov problem. As follows from (6.15), if the initial values q_1, q_2 satisfy the condition $J_{13}q_1 + J_{23}q_2 = 0$, then

$$(\overrightarrow{M_{k+1}})_1 = (\overrightarrow{M_k})_1, \quad (\overrightarrow{M_{k+1}})_2 = (\overrightarrow{M_k})_2, \quad (\overrightarrow{\Omega_k^T M_k \Omega_k})_3 = -(\overrightarrow{M_k})_3,$$

that is, the coadjoint action $M_k \mapsto \Omega_k^T M_k \Omega_k$ is the mirror reflection with respect to the plane $M_3 = 0$. Then it is natural to choose the multiplier λ_k such that $(\bar{M}_{k+1})_3 = (\bar{M}_{k+1})_3$.

As a result, *one of the branches* of the map $\mathcal{B}$ has a one-parametric family of stationary solutions (equilibria) characterized by points of the line

$$\mathbb{P} = \{S^2 \cap \{J_{13}q_1 + J_{23}q_2 = 0\}\}/\mathbb{Z}^2.$$

They correspond to discrete versions of permanent rotations of the body in the classical Suslov problem. (In Figure 6.3 the set of equilibria points is represented by a straight line segment.)

In view of (6.10), opposite points (q_1, q_2, q_0) and $(-q_1, -q_2, q_0)$ on $\mathbb{P}$ correspond to mutually inverse finite rotations Ω and Ω^T respectively.

As also follows from (6.15), there are no equilibria points outside of this line. In particular, neither the saddle points nor the centers of the invariant foliation on $\mathbb{R}P^2$ are stationary points.

Finally, note that, like in the continuous system, for a balanced inertia tensor $J_{13} = J_{23} = 0$ *all* the solutions of (6.15) are stationary, i.e., the discrete body momentum M_k is preserved.

Remark. The foliation of $\mathbb{RP}^2$ by invariant curves gives us a natural way of choosing the branches of the map $\mathcal{B}$ in the general case. Namely, if the initial point (q_1, q_2) lies in the domain $\mathcal{S} \subset \mathbb{RP}^{\in}$ defined by the condition $0 < h \leq h^*$, i.e., it represents either a relatively small or sufficiently big finite rotation Ω, then the points (q_1, q_2) and $(\tilde{q}_1, \tilde{q}_2)$ have to belong to the same connected component of the invariant curve. In other words, if the initial point lies in the interior (exterior) part of $\mathcal{S}$, one has to choose a real solution of (6.16) that has the smallest (largest) norm $\tilde{q}_1^2 + \tilde{q}_2^2$, respectively.

On the other hand, if (q_1, q_2) lies in complement $\mathbb{RP}^2 \setminus \mathcal{S}$, i.e., it is between the separatrices, then a real initial point (q_1, q_2) may lead to complex $(\tilde{q}_1, \tilde{q}_2)$ only. In particular, when the initial point is a center, the next point is necessarily complex, although the value of the integral remains to be real.

If branches of the map $\mathbb{RP}^2 \mapsto \mathbb{RP}^2$ are chosen according to the above way, then the discrete time dynamics inherits all the main properties of the continuous Suslov problem.

Namely, let Δ_- and Δ_+ denote semi-planes of $\mathbb{RP}^2$ defined by conditions $J_{13}q_1 + J_{23}q_2 < 0$ (respectively > 0) and let Θ_- and Θ_+ be semi-planes given by

$$(J_{12}J_{13} + J_{22}J_{23} + J_{23}J_{33})q_1 - (J_{11}J_{13} + J_{12}J_{23} + J_{13}J_{33})q_2 < 0,$$

respectively > 0.

Theorem 6.3. *If the initial point* $\mathbf{q} = (q_1, q_2)$ *lies in the interior part of* $\mathcal{S} \subset \mathbb{RP}^2$*, then for* $k \to -\infty$ *and* $k \to +\infty$ *the sequence* $\{\mathbf{q}_k\}$ *remains on the same branch of invariant curve and tends to the unstable equilibria semi-line* $\mathbb{P}_u = \mathbb{P} \cap \Theta_-$ *and the stable equilibria semi-line* $\mathbb{P}_s = \mathbb{P} \cap \Theta_-$ *respectively. It lies entirely in one of the semi-planes* $\Delta_\pm$*.*

For the foliation indicated in Figure 6.3, the corresponding discrete time dynamics in the neighborhood of the origin is given in Figure 6.4, where stable and unstable equilibria points on $\mathbb{P}$ as depicted as dots and circles respectively.

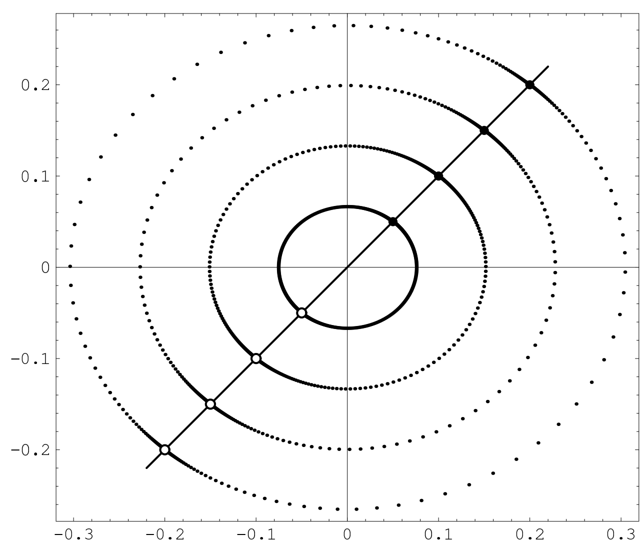

Figure 6.4: Discrete Dynamics near the origin of $\mathbb{RP}^2$.

As follows from Theorem 6.3, for $k \to -\infty$ and $k \to +\infty$ the limit finite rotations Ω_k are mutually inverse. This property gives a perfect discrete analog of limit permanent rotations in the classical Suslov problem.

Proof of Theorem 6.3. First, we describe the discrete dynamics on the part $\mathcal{U}_0$ of the momentum surface $\mathcal{U}$ bounded by the condition

$$E = (J_{11} + J_{33})M_1^2 + 2J_{12}M_1M_2 + (J_{22} + J_{33})M_2^2 \le h^*.$$

For this purpose introduce a new coordinate system

$$\mathcal{M}_1 = (J_{13}(J_{11} + J_{33}) + J_{12}J_{23})M_1 + (J_{23}(J_{22} + J_{33}) + J_{12}J_{13})M_2,$$
$$\mathcal{M}_2 = J_{23}M_1 - J_{13}M_2.$$

In view of relations (6.12) one has

$$\mathcal{M}_1 = (J_{13}q_1 + J_{23}q_2)\left[Q + ((J_{11} + J_{33})(J_{22} + J_{33}) - J_{12}^2)q_0\right], \tag{6.19}$$
$$\mathcal{M}_2 = Qq_0 - (J_{13}q_1 + J_{23}q_2)^2, \tag{6.20}$$
$$Q = (J_{12}J_{13} + J_{22}J_{23} + J_{23}J_{33})q_1 - (J_{11}J_{13} + J_{12}J_{23} + J_{13}J_{33})q_2.$$

Using the properties $(J_{11}+J_{33})(J_{22}+J_{33})-J_{12}^2 > 0$, $q_0 \ge 0$, one can show that in the domain $\mathcal{U}_0$ the expression in square brackets in (6.19) is positive. Hence, on the segment of the line $\mathcal{M}_1 = 0$ in $\mathcal{U}_0$ on has $J_{13}q_1 + J_{23}q_2 = 0$ and it consists of stationary points of the map. The points of $\mathcal{U}_0$ with positive (negative) $\mathcal{M}_1$ correspond to the points on the interior part of $\mathcal{S} \subset \mathbb{RP}^2$ with positive (respectively negative) values of $J_{13}q_1 + J_{23}q_2$. Next, in view of (6.15),

$$\mathcal{M}_{2,k+1} = \mathcal{M}_{2,k} + (J_{13}q_1 + J_{23}q_2)^2,$$

which implies that the coordinate $\mathcal{M}_2$ always increases while the point M_k approaches the line $\mathcal{M}_1 = 0$ along the ellipse $E(M_1, M_2) = \text{const}$. Then, as follows from (6.20), for $k \to -\infty$, one has $\mathcal{M}_2 < 0$, $Q < 0$ and for $k \to \infty$, $\mathcal{M}_2 > 0$, $Q > 0$. As a consequence, the equilibria positions on $\mathbb{P}_u = \mathbb{P} \cap \Theta_-$ are unstable and those on $\mathbb{P}_s = \mathbb{P} \cap \Theta_+$ are stable.

Further, due to (6.15), $\mathcal{M}_{1,k+1} - \mathcal{M}_{1,k} = -(J_{13}q_1 + J_{23}q_2)Q$ and, therefore,

$$\mathcal{M}_{1,k+1} = (J_{13}q_1 + J_{23}q_2)((J_{11} + J_{33})(J_{22} + J_{33}) - J_{12}^2)q_0.$$

The latter and (6.19) implies that, unless $J_{13}q_1 + J_{23}q_2 = 0$, the coordinates $\mathcal{M}_{1,k}$ and $\mathcal{M}_{1,k+1}$ always have the same sign, i.e., the sequence $\{M_k\}$ lies entirely in one of the domains $\mathcal{U}_0 \cap \{\mathcal{M}_1 \lesseqgtr 0\}$. Reformulating these properties for the interior part of the domain $\mathcal{S} \subset \mathbb{RP}^2$, we arrive at the statement of the theorem.

7 Discrete Unbalanced Chaplygin Sleigh

Now we pass to discretization of the EPS equations (5.3) on the coalgebra $se^*(2)$.

The two subsequent positions of the sleigh are given by the matrices

$$X_k = \begin{pmatrix} \cos\theta_k & -\sin\theta_k & x_k \\ \sin\theta_k & \cos\theta_k & y_k \\ 0 & 0 & 1 \end{pmatrix}, \qquad X_{k+1} = \begin{pmatrix} \cos\theta_{k+1} & -\sin\theta_{k+1} & x_{k+1} \\ \sin\theta_{k+1} & \cos\theta_{k+1} & y_{k+1} \\ 0 & 0 & 1 \end{pmatrix}$$

The *helical displacement* in the body frame is defined by $\mathit{\Omega}_k = X_k^{-1}X_{k+1} \in SE(2)$ and straightforward computation shows that

$$\mathit{\Omega}_k = \begin{pmatrix} \cos(\Delta\theta_k) & -\sin(\Delta\theta_k) & \cos\theta_k\,\Delta x_k + \sin\theta_k\,\Delta y_k \\ \sin(\Delta\theta_k) & \cos(\Delta\theta_k) & -\sin\theta_k\,\Delta x_k + \cos\theta_k\,\Delta y_k \\ 0 & 0 & 1 \end{pmatrix}, \tag{7.1}$$
$$\Delta\theta_k = \theta_{k+1} - \cos\theta_k, \quad \Delta x_k = x_{k+1} - x_k, \quad \Delta y_k = y_{k+1} - y_k.$$

Following the expression (3.1), define the left-invariant discrete Lagrangian on $SE(2)\times SE(2)$ by replacing the helical velocity ξ in (5.8) with $X_k^{-1}(X_{k+1}-X_k)$. Up to an additive constant, we get

$$L_d(X_{k+1},X_k)=\frac{1}{2}\mathrm{tr}\,\left(\Omega_k\mathbb{J}\Omega_k^T\right)-\frac{1}{2}\mathrm{tr}\,\left(\mathbb{J}\Omega_k^T+\Omega_k\mathbb{I}\right), \tag{7.2}$$

$$\mathbb{J}=\begin{pmatrix} J/2+ma^2 & mab & ma\\ mab & J2+mb^2 & mb\\ ma & mb & m\end{pmatrix},$$

where, as above, a,b are coordinates of the mass center C in the body frame and J is its scalar moment of inertia with respect to the origin A. This yields the following scalar expression

$$\begin{aligned} L_d =&\frac{m}{2}\Delta y_k^2+\frac{m}{2}\Delta x_k^2+\left(J+ma^2+mb^2\right)(1-\cos\Delta\theta_k)\\ &+am[(\sin\theta_{k+1}-\sin\theta_k)\Delta y_k+(\cos\theta_{k+1}-\cos\theta_k)\Delta x_k]\\ &+bm[(\cos\theta_{k+1}-\cos\theta_k)\Delta y_k-(\sin\theta_{k+1}-\sin\theta_k)\Delta x_k]. \end{aligned} \tag{7.3}$$

In the continuous limit, when

$$\begin{gathered} \Delta\theta_k=\varepsilon\,\omega+O(\varepsilon^2),\quad \Delta x_k=\varepsilon\dot x+O(\varepsilon^2),\quad \Delta y_k=\varepsilon\dot y+O(\varepsilon^2),\qquad \varepsilon<<1,\\ \cos\theta_{k+1}-\cos\theta_k=-\varepsilon\,\omega\sin\theta+O(\varepsilon^2),\quad \sin\theta_{k+1}-\sin\theta_k=\varepsilon\,\omega\cos\theta+O(\varepsilon^2), \end{gathered} \tag{7.4}$$

expression (7.3) divided by ε transforms to the continuous Lagrangian (5.1) plus higher order terms in ε.

According to definition (3.2), the discrete momentum in the body
$P_k=(p_{\theta,k},p_{1,k},p_{2,k})\in se^*(2)$, has the form

$$\begin{aligned} p_{\theta,k}&=-\frac{\partial}{\partial\varepsilon}L_d(\theta_k+\varepsilon,\theta_{k+1},x_k,x_{k+1},y_k,y_{k+1})\Big|_{\varepsilon=0}\\ p_{1,k}&=-\frac{\partial}{\partial\varepsilon}L_d(\theta_k,\theta_{k+1},x_k+\varepsilon\cos\theta_k,x_{k+1},y_k+\varepsilon\sin\theta_k,y_{k+1})\Big|_{\varepsilon=0},\\ p_{2,k}&=-\frac{\partial}{\partial\varepsilon}L_d(\theta_k,\theta_{k+1},x_k-\varepsilon\sin\theta_k,x_{k+1},y_k+\varepsilon\cos\theta_k,y_{k+1})\Big|_{\varepsilon=0}, \end{aligned}$$

that is,

$$\begin{aligned} p_{\theta,k}&=(J+ma^2+mb^2)\sin(\Delta\theta_k)+amV_{2,k}-bmV_{1,k}\,,\\ p_{1,k}&=mV_{1,k}-am(1-\cos(\Delta\theta_k))-bm\sin(\Delta\theta_k),\\ p_{2,k}&=mV_{2,k}+am\sin(\Delta\theta_k)-bm(1-\cos(\Delta\theta_k)), \end{aligned} \tag{7.5}$$

where

$$\begin{aligned} V_{1,k}&=(\Omega_k)_{13}\equiv\Delta x_k\cos\theta_k+\Delta y_k\sin\theta_k,\\ V_{2,k}&=(\Omega_k)_{23}\equiv-\Delta x_k\sin\theta_k+\Delta y_k\cos\theta_k \end{aligned} \tag{7.6}$$

are "discrete velocities" in the body frame.

Next, the coadjoint action on $se^*(2)$ can be written in form

$$\mathrm{Ad}^*_{\Omega_k}P_k=\begin{pmatrix} p_{\omega,k}-p_{2,k}V_{1,k}+p_{1,k}V_{2,k}\\ \cos(\Delta\theta_k)p_{1,k}+\sin(\Delta\theta_k)p_{2,k}\\ -\sin(\Delta\theta_k)p_{1,k}+\cos(\Delta\theta_k)p_{2,k}\end{pmatrix}. \tag{7.7}$$

In the absence of constraints the dynamics of the 2-dimensional body can be represented by the discrete Euler–Poincaré equations

$$P_{k+1}=\mathrm{Ad}^*_{\Omega_k}P_k, \tag{7.8}$$

which gives the momentum conservation law written in the body frame. In particular, for $a = b = 0$ (the mass center C lies at the origin), the system (7.8), (7.7) yields

$$
\begin{aligned}
\sin(\theta_{k+1} - \theta_k) &= \sin(\theta_k - \theta_{k-1}), \\
\Delta x_{k+1} \cos\theta_{k+1} + \Delta y_{k+1} \sin\theta_{k+1} &= \Delta x_k \cos\theta_{k+1} + \Delta y_k \sin\theta_{k+1}, \\
-\Delta x_{k+1} \sin\theta_{k+1} + \Delta y_{k+1} \cos\theta_{k+1} &= -\Delta x_k \sin\theta_{k+1} + \Delta y_k \cos\theta_{k+1},
\end{aligned}
$$

which implies that *for small θ's* the differences $\theta_{k+1} - \theta_k$, $x_{k+1} - x_k$, and $y_{k+1} - y_k$ are the same for any integer k, the result one expects from studying the continuous problem.

Discrete constraint on $SE(2)$. We now impose discrete left-invariant constraints on $SE(2) \times SE(2)$ in the form of restrictions on discrete helical velocities $\Omega_k = X_{k+1} X_k^T$. By analogy with continuous constraint defined by (5.11), a naive choice of a discrete constraint is just to set

$$
(\Omega_k)_{23} \equiv -\sin\theta_k \, \Delta x_k + \cos\theta_k \, \Delta y_k = 0. \tag{7.9}
$$

This choice however is not the right one. Indeed, following our approach to discrete left-invariant constraints, admissible rotations and translations must be exponents of the matrices of the form (5.10). In this case $\mathfrak{h}$ generates the subgroup $SE(n-1)$ and, according to Proposition 3.1, $\exp \mathfrak{d}$ must be a covering of the homogeneous space $SE(n)/SE(n-1)$.

In the particular case $n = 2$, when Ω_k is given by (7.1), we have

Proposition 7.1. *The variety $\mathcal{S} = \exp \mathfrak{d} \subset SE(2)$ is diffeomorphic to the the canonical line bundle $\pi : \mathcal{L} \to \mathbb{R}P^1 = (z_1 : z_2)$ (Moebius cylinder) such that $\pi^{-1}(z_1 : z_2) = \{\nu(z_1, z_2), \nu \in \mathbb{R}\}$ and it is defined by the condition*

$$
\frac{\Omega_{23}}{\Omega_{13}} = \frac{1 - \Omega_{11}}{\Omega_{21}} \, . \tag{7.10}
$$

The latter yields the following constraint

$$
\begin{aligned}
&-(\Delta x_k \cos\theta_k + \Delta y_k \sin\theta_k) \sin(\Delta\theta_k/2) \\
&\qquad + (-\Delta x_k \sin\theta_k + \Delta y_k \cos\theta_k) \cos(\Delta\theta_k/2) = 0
\end{aligned} \tag{7.11}
$$

or, equivalently,

$$
V_{1,k}[1 - \cos(\Delta\theta_k)] - V_{2,k} \sin(\Delta\theta_k) = 0. \tag{7.12}
$$

The corresponding left-invariant constraint on $SE(2) \times SE(2)$ has the form

$$
-\sin\left(\frac{\theta_{k+1} + \theta_k}{2}\right)(x_{k+1} - x_k) + \cos\left(\frac{\theta_{k+1} + \theta_k}{2}\right)(y_{k+1} - y_k) = 0. \tag{7.13}
$$

Observe that in the continuous limit (7.4) this yields the constraint $-\dot{x}\sin\theta + \dot{y}\cos\theta = 0$.

Proof of Proposition 7.1 For an element $S \in \mathfrak{d}$ we have

$$
S = \begin{pmatrix} 0 & -\omega & v \\ \omega & 0 & 0 \\ 0 & 0 & 0 \end{pmatrix}, \quad \exp(St) = \begin{pmatrix} \cos\omega t & -\sin\omega t & \frac{v}{\omega}\sin(\omega t) \\ \sin\omega t & \cos\omega t & \frac{v}{\omega}(1 - \cos(\omega t)) \\ 0 & 0 & 1 \end{pmatrix},
$$

where ω, v are arbitrary. As a result, for the points of the admissible shift subvariety, relation (7.10) holds. Next, since

$$
\omega t = \Delta\theta_k, \quad \text{and} \quad \frac{\Omega_{23}}{\Omega_{13}} \equiv \frac{1 - \cos\omega t}{\sin\omega t} = \tan\frac{\Delta\theta_k}{2}, \tag{7.14}
$$

in view of (7.6), we have (7.11) and (7.12).

Finally, as seen from the last relation, the angle $\Delta\theta_k$ determines the quotient Ω_{23}/Ω_{13}, i.e., a line in $\mathbb{R}^2 = (\Omega_{23}, \Omega_{13})$. As $\Delta\theta_k$ changes by 2π, the line rotates by π, hence $\mathcal{S}$ is diffeomorphic to the Moebius cylinder.

Remark. As seen from relation (7.11), the matrices from $\mathcal{S} \subset SE(2)$ describe "circular translations" of the sleigh along the axis X_k of the blade: the points (x_k, y_k) and (x_{k+1}, y_{k+1}) in $\mathbb{R}^2$ must lie on a circle such that the lines X_k and X_{k+1} are tangent to this circle. This property also implies that

$$\begin{aligned} \Delta x_k \cos\theta_k + \Delta y_k \sin\theta_k &= \Delta x_k \cos\theta_{k+1} + \Delta y_k \sin\theta_{k+1}, \\ -\Delta x_k \sin\theta_k + \Delta y_k \cos\theta_k &= \Delta x_k \sin\theta_{k+1} - \Delta y_k \cos\theta_{k+1} \end{aligned} \tag{7.15}$$

(see Figure 7.1).

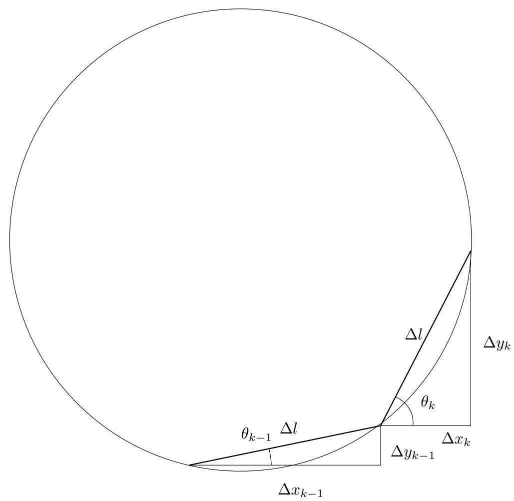

Figure 7.1: The geometry of the incremental displacements for the Chaplygin sleigh.

The above constraint has also the following interpretation: in order to transfer the sleigh from $(\theta_k, x_k, y_k) \in SE(2)$ to $(\theta_{k+1}, x_{k+1}, y_{k+1}) \in SE(2)$ (assuming that this transition is possible), one needs first to perform the rotation over $\Delta\theta_k/2$ at (x_k, y_k), which aims the sleigh towards (x_{k+1}, y_{k+1}), then slide the sleigh from (x_k, y_k) to (x_{k+1}, y_{k+1}), and then perform another rotation over $\Delta\theta_k/2$ (now at (x_{k+1}, y_{k+1})).

Note that under the constraint (7.12) the image of the discrete Legendre transformation (7.5) is an algebraic quartic subvariety $\mathcal{U}$ in $se^*(2) = (p_\theta, p_1, p_2)$ and to a generic pair (p_θ, p_1) there correspond four distinct points on $\mathcal{U}$ and four inverse images on $\mathcal{S} \subset SE(2)$.

Discrete momentum locus $\mathcal{U} \subset se^*(2)$. Below we concentrate on the important case $b = 0$, when the structure of the real surface $\mathcal{U} \subset se^*(2)$ becomes simpler. It is more convenient to describe the image $\tilde{\mathcal{U}}$ of $\mathcal{U}$ in $\mathbb{R}^3 = (p_\theta, \hat{p}_1, z)$, where $\hat{p}_1 = ap_1 + 2ma^2$, $z = \sin(\Delta\theta)$.

Lemma 7.2. *1). For $b = 0$ the surface $\tilde{\mathcal{U}}$ is given by cubic equation*

$$\mathcal{H}(p_\theta, \hat{p}_1, z) = J^2 z^3 - 2Jp_{\theta,k} z^2 + (\hat{p}_1^2 + 2J\hat{p}_1 + p_\theta^2)z - 2p_\theta \hat{p}_1 = 0. \tag{7.16}$$

$\tilde{\mathcal{U}}$ lies entirely between the planes $z = \pm 1$ and is tangent to them along the lines $\ell_\pm = \{\pm p_\theta - \hat{p}_1 = J\}$ respectively. The p_θ- and $\hat{p}_1$-axis belong entirely to $\tilde{\mathcal{U}}$.

2). For the parts of $\tilde{\mathcal{U}}$ over the quadrants

$$\begin{aligned} L_{++} &= \{-\hat{p}_1 + p_\theta > J\} \cap \{-\hat{p}_1 - p_\theta > J\} \quad \text{and} \\ L_{--} &= \{-\hat{p}_1 + p_\theta < J\} \cap \{-\hat{p}_1 - p_\theta < J\} \end{aligned}$$

one has $\cos(\Delta\theta) > 0$, i.e., $-\pi/2 < \Delta\theta < \pi/2$ and in the rest of quadrants one has $\cos(\Delta\theta) < 0$ $(\pi/2 < \Delta\theta < 3\pi/2)$.

3). The projection $\Pi : \tilde{U} \to \mathbb{R}^2 = (p_\theta, \hat{p}_1)$ *is one-to-one except the above segments and the interior of triangular domain bounded by the discriminant curve*

$$\hat{p}_1^4 + 6J\hat{p}_1^3 + \hat{p}_1^2(12J^2 + 2p_\theta^2) - \hat{p}_1(10Jp_\theta^2 - 8J^3) + p_\theta^4 - J^2p_\theta^2 = 0.$$

The curve is symmetric with respect to $\hat{p}_1$*-axis, it is tangent to* p_θ*-axis at the origin* $(0,0)$ *and has 3 cusp points with coordinates* $(0,-2J)$, $(c_1,c_2), (-c_1,c_2)$, *with some positive constants* c_1, c_2. *In this domain the projection* Π *is 3 to 1.*

4). The curve $\{V_1 = 0\} \subset \tilde{\mathcal{U}}$ *is projected onto the ellipse*

$$\mathcal{E} = \{p_\theta = (J + ma^2)\sin(\Delta\theta), \quad \hat{p}_1 = ma^2(1 + \cos(\Delta\theta)) \mid \Delta\theta \in (0; 2\pi)\}. \qquad (7.17)$$

Inside the ellipse the values of V_1 *are negative and outside are positive.*

Note that the point O with coordinates $p_\theta = 0$, $\hat{p}_1 = 2ma^2$ corresponds to the origin in the (p_θ, p_1) phase plane and in a neighborhood of this point the projection Π is one-to-one. An example of the surface $\tilde{\mathcal{U}}$ for $J = 1.5$ is presented in Figure 7.2.

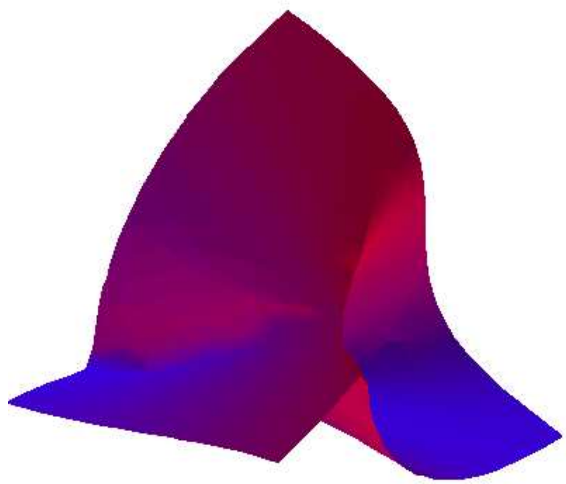

Figure 7.2: The surface $\tilde{\mathcal{U}}$.

Proof of Lemma 7.2. 1). Using the condition (7.12), we exclude V_1, V_2 from the first two equations of (7.5) to obtain the following condition on $\Delta\theta_k$,

$$J\sin^2(\Delta\theta_k) - p_{\theta,k}\sin(\Delta\theta_k) + (2ma^2 + ap_{1,k})[1 - \cos(\Delta\theta_k)] = 0. \qquad (7.18)$$

This equation always has trivial solution $\Delta\theta_k = 2n\pi$, $n \in \mathbb{Z}$. Setting $z = \sin(\Delta\theta_k)$, $\cos(\Delta\theta_k) = \sqrt{1 - z^2}$, $\hat{p}_1 = ap_x + 2ma^2$, we arrive at a quartic polynomial equation with respect to z, which has the root $z = 0$. Factoring it out and omitting the index k, one gets the cubic equation (7.16).

Now setting in (7.16) $z = \pm 1$, we get $(J \mp p_\theta + \hat{p}_1)^2 = 0$, which implies that $\tilde{\mathcal{U}}$ is indeed tangent to the planes $z = \pm 1$ along the lines $\ell_\pm$. Finally, setting $z = p_\theta = 0$ or $z = \hat{p}_1 = 0$, one sees that equation (7.16) is satisfied for any $\hat{p}_1$ and p_θ respectively.

2). For fixed $p_\theta, \hat{p}_1$, each root of (7.16) gives a solution of (7.18) with a sign of $\cos(\Delta\theta_k)$ appropriately chosen. As seen from (7.18), for large $|p_x|$ and small $z = \sin(\Delta\theta)$, the value of $\cos(\Delta\theta)$ must be close to 1, whereas for large $p_\theta > 0$ and small $|p_x|$, $\cos(\Delta\theta)$ must be negative. Since the sign of $\cos(\Delta\theta)$ can change only under passage from one quadrant on the plane (p_θ, Y) to another one, this proves item 2).

Items 3), 4) are verified by direct calculations.

Discrete dynamics on $se^*(2)$ with the constraint. According to (3.8), the discrete Euler–Poincaré–Suslov equations associated with the constraint (5.11) have the form

$$P_{k+1} = \mathrm{Ad}^*_{\Omega_k} P_k + \lambda_k (0,0,1)^T. \tag{7.19}$$

Substituting here expressions (7.7), we find that under the constraint (7.12) the first two components of P_{k+1} have the form

$$\begin{aligned} p_{\theta,k+1} &= (J + ma^2 + mb^2)\sin(\Delta\theta_k) - bmV_{1,k} \\ &\quad + am[-\Delta x_k \sin\theta_{k+1} + \Delta y_k \cos\theta_{k+1}], \\ p_{1,k+1} &= mV_{x,k} - bm\sin(\Delta\theta_k) \\ &\quad + am[\Delta x_k \cos\theta_{k+1} + \Delta y_k \sin\theta_{k+1}], \end{aligned}$$

which, in view of (7.15), (7.5), yields

$$\begin{aligned} p_{\theta,k+1} &= p_{\theta,k} - 2amV_{2,k}\,, \\ p_{1,k+1} &= p_{1,k} + 2am(1-\cos(\Delta\theta_k))\,. \end{aligned} \tag{7.20}$$

Expressions (7.20), (7.12) define a multi-valued map $\mathcal{U} \to \mathcal{U}$ or $\mathcal{S} \to \mathcal{S}$ which consists of 3 steps:

1). Given $\Delta\theta_k, V_{1,k}$, one finds $V_{2,k}$ form the constraint (7.12) and then $p_{\theta,k}, p_{1,k}, p_{2,k}$ from the Legendre transformation (7.5).

2). One finds $p_{\theta,k+1}, p_{2,k+1}$ from (7.20).

3). One finds $\Delta\theta_{k+1}, V_{1,k+1}$ by choosing a solution of the system of equations

$$\begin{aligned} p_{\theta,k+1} &= (J + ma^2 + mb^2)\sin(\Delta\theta_{k+1}) + \left(am\frac{1-\cos(\Delta\theta_{k+1})}{\sin(\Delta\theta_{k+1})} - bm \right) V_{x,k+1}\,, \\ p_{1,k+1} &= mV_{x,k+1} - am(1-\cos(\Delta\theta_{k+1})) - bm\sin(\Delta\theta_{k+1}), \end{aligned}$$

which are obtained from (7.5), (7.12) by replacing $k \to k+1$.

Theorem 7.3. *Equations (7.20) preserve the quantity*

$$E = mp_\theta^2 + 2bmp_\theta p_1 + (J + m(a^2+b^2))p_1^2, \tag{7.21}$$

which coincides with the truncated energy integral (5.5) of the continuous Chaplygin sleigh.

Proof. Substituting expressions (7.5) and (7.20) into (7.21) and taking into account the constraint (7.12), one obtains the same expression in terms of $\Delta\theta_k, V_{1,k}$ and $V_{2,k}$.

Since the quadratic form (7.21) is positive definite, we conclude that the invariant manifolds of the map (7.20) are the ellipses in the $p_\theta p_1$-plane.

Stationary solutions of the discrete Chaplygin sleigh. As follows from (7.20), for the initial conditions $\{\Delta\theta_k = 0, V_{2,k} = 0\}$ one has

$$p_{\theta,k+1} = p_{\theta,k}, \quad p_{1,k+1} = p_{1,k}.$$

Hence, it is natural to choose such λ_k in (7.19) that $p_{2,k+1} = p_{2,k}$ as well. Thus, like the continuous system (5.4), for $a \neq 0$ the map (7.19) has a family of stationary solutions which, on the momenta plane (p_θ, p_1), is represented by the line $\{p_\theta + bp_1 = 0\}$. Such solutions correspond to shifts in the (x, y)-plane along the axis of the blade by constant distances.

On the other hand, for $a = 0$ all the solutions are stationary. That is, in contrast to the case of absence of constraints, when the discrete momentum in space is preserved, now it is the momentum in the body P, which is preserved. In view of (7.5), this implies

$$\Delta\theta_{k+1} = \Delta\theta_k, \quad V_{1,k+1} = V_{1,k}.$$

As a result, the discrete trajectory on the plane (x, y) consists of displacements along a circle with radius $\rho = V_{1,k}/\sin(\Delta\theta_k)$ [5] . The same behavior occurs to the continuous sleigh for $a = 0$.

[5]As numerical simulations show, if one chooses the naive constraint (7.9) instead of (7.10), then for $a = 0$ the discrete trajectory on the plane (x, y) lies on a spiral.

The case $b = 0$, $a \neq 0$. In this case the map $(p_{\theta,k}, p_{x,k}) \to (p_{\theta,k+1}, p_{1,k+1})$ has a line of stationary points $p_\theta = 0$, and, according to Theorem 7.3, the discrete trajectories lie on symmetric invariant ellipses $mp_\theta^2 + (J + ma^2)p_1^2 = E$. Without loss of generality, we assume $a > 0$. Then the following property holds.

Theorem 7.4. *In the neighborhood of the origin O bounded by the condition $E < m^2a^2(J+ma^2)$ the map is single-valued and has a bi-asymptotic behavior similar to that of the continuous Chaplygin sleigh system. Namely, for $k \to -\infty$, the point $(p_{\theta,k}, p_{x,k})$ approaches, along the corresponding invariant ellipse, a point of the segment $\{p_\theta = 0, \ -ma < p_1 < 0\}$ of unstable stationary points, and for $k \to +\infty$, the point $(p_{\theta,k}, p_{x,k})$ approaches one of the points of the segment $\{p_\theta = 0, \ 0 < p_1 < ma\}$ of stable stationary points. In both cases the sequence $\{(p_{\theta,k}, p_{x,k})\}$ remains in one of the half-planes $p_\theta < 0$ or $p_\theta > 0$.*

Proof. Part (3) of Lemma 7.2 implies that the map is single-valued in the region $E < m^2a^2(J + ma^2)$.

Next, as follows from the first relation in (7.20) for $a > 0$, the increment $p_{1,k+1} - p_{1,k}$ is always greater than or equal to zero. Then, to prove the bi-asymptotic behavior, it remains only to show that the sequence $\{(p_{\theta,k}, p_{1,k})\}$ lies entirely in one of the half-planes $p_\theta \lesseqgtr 0$.

Indeed, let the point $(p_{\theta,k}, p_{x,k})$ be inside the ellipse $\mathcal{E}$ given by (7.17). First, assume that $p_{\theta,k} > 0$. Then, in view of items (2), (4) of Lemma 7.2, and the constraint (7.11), $V_{1,k}$ and $V_{2,k}$ are negative. According to (7.20), the increment $p_{\theta,k+1} - p_{\theta,k}$ is then positive. Similarly, for $p_{\theta,k} < 0$ one has $p_{\theta,k+1} - p_{\theta,k} < 0$.

Next, if $0 < p_{1,k} < ma$ and $(p_{\theta,k}, p_{x,k})$ lies in the domain $E < (J + ma^2)m^2a^2$, then, using (7.5), (7.11), one shows that $2amV_{2,k} > p_{\theta,k}$ for $p_{\theta,k} > 0$ and $2amV_{2,k} < p_{\theta,k}$ for $p_{\theta,k} < 0$. Therefore, in view of (5.3), $p_{\theta,k+1} > 0$, respectively, $p_{\theta,k+1} < 0$.

As a result, in any case, $p_{\theta,k}$ and $p_{\theta,k+1}$ cannot have different signs, which proves the theorem.

One concludes that in the neighborhood of the origin O the discrete-time dynamics is similar to that of the Suslov problem illustrated in Figure 6.4.

We conclude this section with an example of the discrete sleigh trajectory on the plane (x, y) compared to a continuous trajectory for $b = 0$ with a cusp, as presented in Figure 7.3.

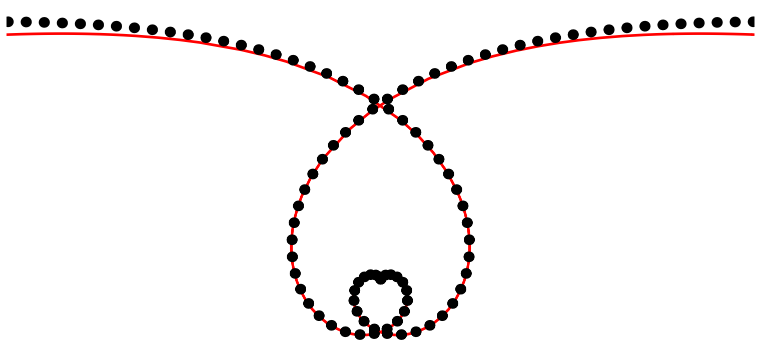

Figure 7.3: A typical discrete sleigh trajectory.

8 Conclusions

The discrete nonholonomic Suslov problem and the Chaplygin sleigh that we introduced in this paper properties of their corresponding continuous-time dynamical systems; in particular, they preserve the reduced constrained energy and, in the balanced case, the momentum. This enables one to obtain explicit solutions for the momentum dynamics of both discrete systems in terms of theta-functions and exponents. It is not currently clear if the complete solvability is due to the (low) dimension of the systems and if it is possible to construct completely solvable discretizations of the multidimensional Suslov and Chaplygin problems. These issues will be addressed in a future publication.

On the other hand, by modifying our approach, one can also consider discretizations of nonholonomic LR systems on Lie groups. For such systems, the Lagrangian is left-invariant while the constraint distribution is *right*-invariant. The discrete dynamics of such systems, as well as the existence of their invariant measure, is currently being developed and will be exposed in a future publication.

Acknowledgments

YNF's research was partially supported by Spanish Ministry of Science and Technology grant BFM 2003-09504-C02-02; DVZ's research was partially supported by NSF grant DMS-0306017.

References

[1] Arnold, V. I., V. V. Kozlov, and A. I. Neishtadt [1989], Mathematical Aspects of Classical and Celestial Mechanics. *Dynamical System III*, Springer-Verlag, New York.

[2] Bloch, A. M. [2003], *Nonholonomic Mechanics and Control*, Interdisciplinary Applied Mathematics **24**, Springer-Verlag.

[3] Bloch A. M., P. S. Krishnaprasad, J. E. Marsden, and R. Murray [1996], Nonholonomic Mechanical Systems with Symmetry. *Arch. Rational Mech. Anal.* **136**, 21–99.

[4] Bobenko A. I. and Y. B. Suris [1999], Discrete Lagrangian Reduction, Discrete Euler–Poincar Equations, and Semidirect Products. *Lett. Math. Phys.* **49**, 79–93.

[5] Chaplygin, S. A. [1911], On the Theory of Motion of Nonholonomic Systems. The Theorem on the Reducing Multiplier, *Math. Sbornik* **XXVIII**, 303–314, (in Russian).

[6] Cortés J. and Martínez S. [2001], Nonholonomic Integrators. *Nonlinearity* **14**, 1365–1392.

[7] Fedorov Yu. N. and V. V. Kozlov [1995], Various Aspects of n-Dimensional Rigid Body Dynamics. *Amer. Math. Soc. Transl* **168**, 141–171.

[8] Gray, A. [1997], *Modern Differential Geometry of Curves and Surfaces with Mathematica,* 2nd ed., Boca Raton, FL: CRC Press.

[9] Jovanović, B. [2001], Geometry and Integrability of Euler–Poincaré–Suslov Equations. *Nonlinearity* **14**, 1555–1657.

[10] Helgason, S. [1962] Differential Geometry and Symmetric Spaces. Academic Press, New York.

[11] Kozlov, V. V. [1985], On the Integration Theory of Equations of Nonholonomic Mechanics. *Advances in Mechanics* **8**, 85–107 (in Russian).

[12] Kozlov, V. V. [1988] Invariant Measures of the Euler–Poincaré Equations on Lie algebras. *Funct. Anal. Appl.* **22**, 58–59.

[13] de León, M., D. Martín de Diego, and A. Santamaría Merino. [2002] Geometric Integrators and Nonholonomic Mechanics. arXiv:math-ph/0211028.

[14] McLachlan, R. [1993], Explicit Lie–Poisson Integration and the Euler Equations, *Phys. Rev. Lett.* **71**, 3043–3046.

[15] Marsden, J. E., S. Pekarsky, and S. Shkoller [1999], Discrete Euler–Poincaré and Lie–Poisson Equations. *Nonlinearity* **12**, 1647–1662.

[16] Marsden, J E. and T. S. Ratiu [1999], *Introduction to Mechanics and Symmetry,* Texts in Applied Mathematics **17**, Springer-Verlag.

[17] Marsden, J. E. and M. West [2001], Discrete mechanics and variational integrators, *Acta Numerica*, 357–514.

[18] Moser, J. and A. Veselov [1991], Discrete Versions of Some Classical Integrable Systems and Factorization of Matrix Polynomials. *Comm. Math. Phys.* **139**, 217–243.

[19] Neimark, Ju. I. and N. A. Fufaev [1972] *Dynamics of Nonholonomic Systems.* Translations of Mathematical Monographs **33**, AMS, Providence.

[20] *Steiner's Roman Surface.* http://mathworld.wolfram.com/RomanSurface.html

[21] Suslov, G. *Theoretical Mechanic*, Vol. 2, Kiev (in Russian).

[22] Veselov, A. P., [1988], Integrable Discrete-Time Systems and Difference Operators, *Funk. Anal. Appl.* **22**, 1–13.

[23] Veselov, A. P., [1991], Integrable Lagrangian Correspondences and the Factorization of Matrix Polynomials, *Funk. Anal. Appl.* **25**, 38–49.

[24] Wendland, J. M, and J. E. Marsden [1997], Mechanical Integrators Derived from a Discrete Variational Principle, *Physica D* **106**, 223–246.

[25] Whittaker, E. T. [1960] *A Treatise on Analytical Dynamics,* 4th ed., Cambridge Univ. Press, Cambridge.

[26] Zenkov, D. V. and A. M. Bloch [2000], Dynamics of the n-Dimensional Suslov problem. *J. Geom. Phys.* **34**, 121–136.

[27] Zenkov, D. V. and A. M. Bloch [2003], Invariant Measures of Nonholonomic Flows with Internal Degrees of Freedom. *Nonlinearity* **16**, 1793–1807.

[28] Zenkov, D. V. [2003], Linear Conservation Laws of Nonholonomic Systems with Symmetry. *Discrete and Continuous Dynamical Systems (extended volume)*, 963–972.